

Pre-Trained Denoising Autoencoders Long Short-Term Memory  
Networks as probabilistic Models for Estimation of Distribution  
Genetic Programming

---

Student: Roman Höhn

Date of Birth: 1991-04-14

Place of Birth: Wiesbaden, Hesse

Student ID: 2712497

Supervisor: David Wittenberg

---

Master Thesis - M.Sc. Business Education

FB 03: Chair of Business Administration and Computer Science

Johannes Gutenberg University Mainz

Date of Submission: 2023-02-08

# Contents

|   |           |
|---|-----------|
| <b>Abstract</b>   | <b>3</b>  |
| <b>1 Introduction</b>   | <b>3</b>  |
| <b>2 Theoretical Foundations</b>  | <b>3</b>  |
| 2.1 Denoising Autoencoder Genetic Programming . . . . .                 | 3         |
| 2.1.1 Evolutionary Computation . . . . .                                | 3         |
| 2.1.2 Genetic Programming . . . . .                                     | 4         |
| 2.1.3 Estimation of Distribution Algorithms . . . . .                   | 4         |
| 2.1.4 EDA-GP . . . . .  | 4         |
| 2.1.5 Denoising Autoencoders . . . . .                                  | 4         |
| 2.2 Pre-Training . . . . .  | 5         |
| <b>3 Pre-Training in DAE-GP</b>   | <b>5</b>  |
| 3.1 Implementation . . . . .  | 6         |
| 3.2 Benchmark Problem . . . . .   | 9         |
| <b>4 Results for the Airfoil Dataset</b>                                | <b>10</b> |
| 4.1 Influence on Generalisation . . . . .                               | 10        |
| 4.2 Influence on solution quality . . . . .                             | 13        |
| 4.2.1 Dynamic Adjustment of Hidden Neurons . . . . .                    | 17        |
| 4.2.2 Reduced Number of Hidden Layers . . . . .                         | 19        |
| 4.2.3 Alternative Pre-Training Strategies . . . . .                     | 21        |
| 4.3 Influence on Run-Time . . . . .                                     | 23        |
| <b>5 Results over different Real-World Symbolic Regression Problems</b> | <b>29</b> |
| 5.1 Influence on Fitness . . . . .                                      | 30        |
| 5.2 Influence on Solution Size . . . . .                                | 32        |
| 5.3 Influence on Population Diversity . . . . .                         | 33        |
| 5.4 Influence on the number of Training epochs per Generation . . . . . | 34        |
| <b>6 Conclusion and Discussion</b>                                      | <b>35</b> |
| 6.1 Benefits of using Pre-Training . . . . .                            | 35        |
| 6.2 Disadvantages of using Pre-Training . . . . .                       | 35        |
| 6.3 Limitations and open Questions . . . . .                            | 36        |
| <b>Nomenclature</b>   | <b>37</b> |
| Symbols . . . . .   | 37        |
| Abbreviations . . . . .   | 37        |
| <b>References</b>   | <b>38</b> |
| <b>Statutory Declaration</b>  | <b>41</b> |

## List of Tables

|    |  |    |
|----|--|----|
| 1  | GP - Hyperparameter  | 9  |
| 2  | DAE-LSTM - Hyperparameter  | 9  |
| 3  | Airfoil - Dataset Description  | 10 |
| 4  | Real World Symbolic Regression Benchmark Problems                                      | 29 |
| 5  | Median Best Fitness after 30 generations - Real World Symbolic Regression              | 31 |
| 6  | Median Size of the best solution after 30 generations - Real World Symbolic Regression | 33 |
| 7  | Median Population Diversity over 30 Generations - Symbolic Regression                  | 34 |
| 8  | Median Number of Training Epochs per Generation - Symbolic Regression                  | 35 |
| 9  | List of Mathematical Symbols   | 37 |
| 10 | List of Abbreviations  | 37 |

## List of Figures

|    |  |    |
|----|--|----|
| 1  | Regular DAE-GP Flowchart   | 7  |
| 2  | Pre-Trained DAE-GP Flowchart   | 8  |
| 3  | First Generation Median Reconstruction Error for variable number of hidden Neurons                         | 12 |
| 4  | First Generation Median Reconstruction Error for variable number of hidden Layers                          | 13 |
| 5  | Best Fitness over 30 Generations - Airfoil   | 14 |
| 6  | Best Fitness after 30 Generations - Airfoil  | 15 |
| 7  | Median Solution Size over 30 Generations - Airfoil   | 16 |
| 8  | Median Population Diversity over 30 Generations - Airfoil  | 17 |
| 9  | Median Number of trainable Parameters over 30 Generations - Airfoil - Dynamic adjustment of regular DAE-GP | 18 |
| 10 | Median Best Fitness over 30 Generations - Airfoil - Dynamic adjustment of regular DAE-GP                   | 19 |
| 11 | Fitness over 30 Generations - Airfoil - Single Hidden Layer  | 20 |
| 12 | Fitness after 30 Generations - Airfoil - Single Hidden Layer   | 21 |
| 13 | Best Fitness over 30 Generations - Airfoil - Alternative Pre-Training Strategies                           | 22 |
| 14 | Best Fitness on Test Set after 30 Generations - Airfoil - Alternative Pre-Training Strategies              | 23 |
| 15 | Median Runtime - Airfoil   | 24 |
| 16 | Total Runtime Boxplot - Airfoil  | 25 |
| 17 | Median Number of Training Epochs per Generation - Airfoil  | 26 |
| 18 | Median Sampling Time per Generation - Airfoil  | 27 |
| 19 | Median Runtime excluding Time for Sampling - Airfoil   | 28 |
| 20 | Cumulative Time consumption by Function Calls (Top 20) - Airfoil   | 29 |
| 21 | Fitness over 30 Generations - Real World Symbolic Regression   | 30 |
| 22 | Fitness after 30 Generations - Real World Symbolic Regression  | 31 |
| 23 | Size of the best Solution over 30 Generations - Real World Symbolic Regression                             | 32 |
| 24 | Population Diversity over 30 Generations - Real World Symbolic Regression                                  | 33 |
| 25 | Training Epochs over 30 Generations - Real World Symbolic Regression                                       | 34 |

# Abstract

...

## 1 Introduction

Denoising Autoencoder Genetic Programming (DAE-GP) is a novel variation of an genetic programming based Estimation of Distribution Algorithm (EDA-GP) that uses a denoising autoencoders long short-term memory network (DAE-LSTMs) as a probabilistic model to sample new candidate solutions [33].

DAE-LSTMs are artificial neural networks that can be trained in an unsupervised learning environment to minimize a reconstruction error for encoding input data into a compressed representation and subsequently decoding the compressed representation back to the input dimension. In DAE-GP, DAE-LSTMs are trained with a subset of high-fitness solutions selected from a parent population with the aim to capture their promising qualities. The resulting model is then used to sample new offspring solutions by propagating partially mutated solutions from the parent population through the DAE-LSTMS [33]. In previous work DAE-GP has been shown to outperform GP for both a generalized version of the royal tree problem [33] as well as for a real-world symbolic regression problem [32].

The DAE-GP algorithm first described by [33] trains a DAE-LSTMs for each generation  $g$  of the search from scratch. [32] and [31] suggests the incorporation of a pre-training strategy into the evolutionary search as a possible way of improving the overall performance of the DAE-GP algorithm. The key idea is to pre-train an initial DAE-LSTM on a large population of candidate solutions and to use the pre-trained parameters of this initial model in each generation of the search as starting parameters for the current generation DAE-LSTM. This thesis studies the influence of using pre-trained DAE-LSTMs in DAE-GP for symbolic regression, especially looking at the influence on overall quality of solutions found by DAE-GP and effects on run-time. The aim of this study is to answer the question if a pre-training strategy can be used to improve DAE-GP and to study both positive and negative effects on overall performance.

...

## 2 Theoretical Foundations

*This section describes the relevant concepts that are necessary for the understanding and classification of DAE-GP as well as the concept of pre-training in artificial neural networks*

### 2.1 Denoising Autoencoder Genetic Programming

DAE-GP is an EDA-GP algorithm that uses DAE-LSTM networks as a probabilistic model to sample new offspring solutions [33].

#### 2.1.1 Evolutionary Computation

As a variant of GP, DAE-GP can be classified as a meta-heuristic that belongs to the field of evolutionary computation (EC). EC based meta-heuristics are optimization methods that simulate the process of Darwinian evolution to search for high quality solutions by applying selection and

variation operators to a population of candidate solutions. Examples of EC include genetic algorithms (GA), evolutionary strategies (ES) and GP. In EC, the quality of a solution is commonly measured as fitness and the time steps of the search are called generations. Another important concept in EC is the distinction between genotypes and phenotypes of solutions, the genotype contains the information that is necessary to construct the phenotype, the outer appearance of a particular solution on which we measure the overall quality of solutions. The representation of a solution is therefore defined by the mapping of genotypes to phenotypes [22]. Genetic operators, such as mutation or recombination are usually applied to the genotype of solutions.

### 2.1.2 Genetic Programming

GP follows the same basic evolutionary principle of EC but searches for more general, hierarchical computer programs of dynamically varying size and shape [14]. The computer programs that are at the center of the evolutionary search in GP are commonly represented by tree structures at the level of their phenotype [22]. Since GP searches for high fitness computer programs that produce a desired output for some input, it can be applied to various different problem domains such as symbolic regression, automatic programming, or evolving game-playing strategies [14]. An important quality of GP is the ability to search for solutions of variable length and structure. GP is an especially useful meta heuristic for problems where no a priori knowledge about the final form of good solutions is available. GPs ability to optimize solutions for their structure as well as for their parameters led to it being one of the most prevalent methods used for symbolic regression [19].

### 2.1.3 Estimation of Distribution Algorithms

The aim of Estimation of distribution algorithms (EDA) is to replace the standard variation operators used in GA by building probabilistic models that can capture complex dependencies between different decision variables of an optimization problem [22]. EDAs use this probabilistic model to sample new offspring solutions inside an evolutionary search to replace crossover and/or mutation operators.

### 2.1.4 EDA-GP

... insert some smart stuff here...

### 2.1.5 Denoising Autoencoders

One possible way of model building in EDA proposed by [21] is to use denoising autoencoders (DAEs) as generative models to capture complex probability distributions of decision variables. DAE, a variation of the autoencoders (AE), are a widely used type of neural networks in the domain of unsupervised machine learning that maps  $n$  input variables to  $n$  output variables using a hidden representation.

AE were introduced by [10] to compress high-dimensional data into lower-dimensions. An AE consists of two different sub-units:

- Encoder  $g(x)$ : Encode input data to a smaller central layer  $h$
- Decoder  $d(h)$ : Decode and output the the encoded data back to its original dimension

The AE is trained to reduce the reconstruction error between input and output data, after the training procedure is finished the network is able to reduce the dimensional of input data to a compressed representation[10].

DAE was first introduced by [27] as an improved AE with the ability to learn new representations of data that is especially robust to partially corrupted input data. DAE modifies the AE by using partially corrupted input data for the AE and training it to reconstruct the uncorrupted, original version of the input data.

Since the hidden representation of DAE captures the dependency structure of the input data it can therefore also be used to generate new solutions in the context of GAs [21].

DAE-GP builds upon the concept of using DAEs in EDAs described by [21] and transfers the concept to the domain of GP. The mutation and crossover operators of standard GP are replaced by sampling new solutions from a probabilistic model that is build by training a DAEs long short-term memory (LSTM) network on a subset of high fitness solutions from the current population [33].

LSTMs are a variant of artificial neural networks first introduced by [11] that can store learned information over an extended time period while avoiding the problem of vanishing and/or exploding gradients. Since DAE-GP encodes candidate solutions as linear strings in prefix notation, the DAE in DAE-GP uses LSTMs for both encoding and decoding where the total amount of time steps  $T$  is equal to sum of the length of the input solution and the output solution [33].

## 2.2 Pre-Training

Pre-Training describes the concept of initially training an artificial neural network on a large dataset before using it to solve a more specific task. It is a commonly used strategy in deep architectures that has been shown to improve both the optimization process itself as well as the generalization behavior if compared to the standard approach of using randomly initialized parameters [5].

The strategy of pre-training artificial neural networks is based on the idea of transfer learning that aims at retaining previously learned knowledge from one task to re-use it for another task [7] [18]. Transfer learning traditionally follows a two phase approach:

1. Pre-Training Phase: Capture knowledge from source task
2. Fine-Tuning Phase: Transfer knowledge to the target task

where source task and target task are usually similar but may differ in their feature space and the distribution of training data [18].

Some of the main motivations for using pre-training is the ability to reduce the need for large amounts of training data which can often be unavailable or too expensive to collect as well as an improved performance by either reducing the computational effort that is necessary to train a model to solve a specific task or by improving the models generalization ability.

... describe different pre-training strategies, e.g. few shot, perpetual, re-using...

- describe unsupervised vs supervised pre-training...

## 3 Pre-Training in DAE-GP

The pre-training strategy used in this thesis is applied to the DAE-LSTM model  $M_g$  that are used in each DAE-GP generation  $g$  for  $g \in 1, \dots, g_{max}$ . Instead of initializing and optimizing each model from scratch as done in previous work (e.g. [33] [32]), a separate DAE-LSTM network  $\hat{M}$  will be trained on a large population of randomly initialized solutions.

The trainable parameters  $\theta_{\hat{M}}$  obtained after finishing the training procedure of  $\hat{M}$  are then used as the starting parameters for each following DAE-LSTM model  $M_g$  for  $g \in 1, \dots, g_{max}$ .

The motivation for incorporating pre-training into DAE-GP is based on the following suspected mechanisms of improvement:

1. Improve overall performance of DAE-GP by improving either run time and/or solution quality
2. Reduce the need for large population sizes to avoid sampling error
3. Improve model robustness and generalization ability

The probably most obvious motivation for using a pre-training strategy in DAE-GP is based on the fact, that initializing  $M_g$  with pre-trained weights  $\theta_{\hat{M}}$  is likely to reduce the amount of training epochs that are necessary until the point of training error convergence is reached.

Early research on pre-training for DAE by [5] comes to the conclusion that besides adding robustness to models the strategy also results in improved generalization and better performing models. The authors describe that unsupervised pre-training behaves like a regularizer on DAE networks, the mean test error and it's variance are reduced for DAE networks that are initialized from pre-trained weights if compared to the same architectures that use random initialization.

Another important finding by [5] is that the positive effect of pre-training is dependent on both the depth of the network as well as the size of layers - while increasingly larger networks benefit increasingly more from pre-training the final performance of small architectures tends to be worse with pre-training than with randomized weight initialization. The authors find evidence that pre-training DAE is especially useful for optimizing the parameters of the lower layers of the network.

Another motivation for introducing pre-training into DAE-GP is the prevalence of sampling error for small GP populations sizes. [23] finds that sampling error, non-systematic errors that are caused by observing only a small subset of the statistical population, is a severe problem in the domain of GP since the initial population may not be a representative sample of all possible solutions. [23] also introduces a method for calculating optimal population sizes to minimize the presence of sampling error. Since DAE-LSTM of DAE-GP learns the properties of it's training population and reuses the acquired knowledge in the sampling procedure, using the parameters obtained from training  $\hat{M}$  on a sufficiently large training population might reduce the need for large population sizes in the following generations of the search if  $\hat{M}$  already implicitly captured the properties of a representative sample of solutions. If this mechanism can be applied successfully it would benefit the performance of DAE-GP by increasing the population diversity (resulting in better solution quality) as well as by reducing the need for large population sizes which require computational resources.

### 3.1 Implementation

The DAE-GP algorithm, first described by [33], is summarized as a flowchart in figure 1. After setting the generation counter  $g$  to 0 and creating the initial population of solutions  $P_0$ , DAE-GP enters the main loop that checks if a termination criteria is satisfied (i.e. maximum number of generations or fitness evaluations is reached). For each generation  $g$  the fitness of all new individuals in  $P_g$  is evaluated. During model building, DAE-GP selects a subset  $X_g$  of the current population that is used as training data for the DAE-LSTM model  $M_g$  which is trained to learn the properties of  $X_g$ . The trained model  $M_g$  is then used for model sampling, partially mutated solutions from  $P_G$  are propagated through  $M_g$  to create a new population  $P_{g+1}$ . This process is repeated until the termination criteria is met and DAE-GP returns the highest fitness solutions.

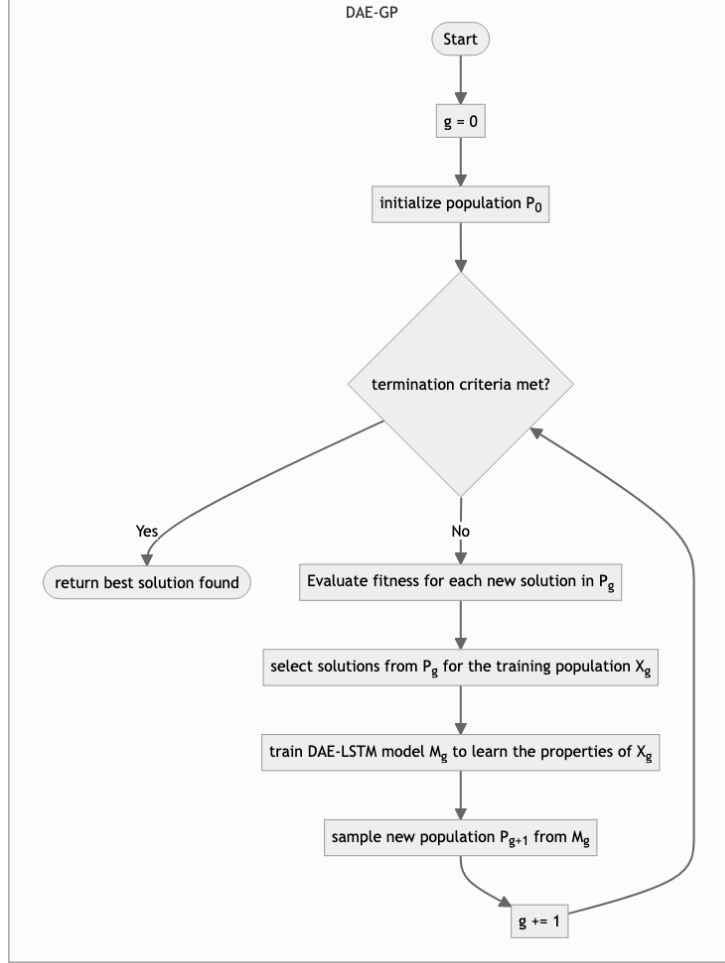


Figure 1: Regular DAE-GP Flowchart

The pre-training strategy implemented for all experiments in this thesis is visualized as another flowchart in figure 2. The main difference to regular DAE-GP is the inclusion of an initial pre-training phase where a separate population  $\hat{P}$  is first initialized and then randomly split by half into  $\hat{P}_{train}$  and  $\hat{P}_{test}$ . A DAE-LSTM model  $\hat{M}$  is then trained to learn the properties of  $\hat{P}_{train}$  using an early stopping training mode where we stop training as soon as the validation error for  $\hat{P}_{test}$  converges. After the training for  $\hat{M}$  is stopped, the current state of  $\hat{M}$  is frozen and the optimized trainable parameters  $\theta_{\hat{M}}$  are saved before terminating the pre-training phase to start the DAE-GP phase. During the DAE-GP phase, the only difference to the traditional DAE-GP algorithm described in figure 1 is during model building: We initialize  $M_g$  with  $\theta_{\hat{M}}$  before training it to learn the properties of  $X_g$ .

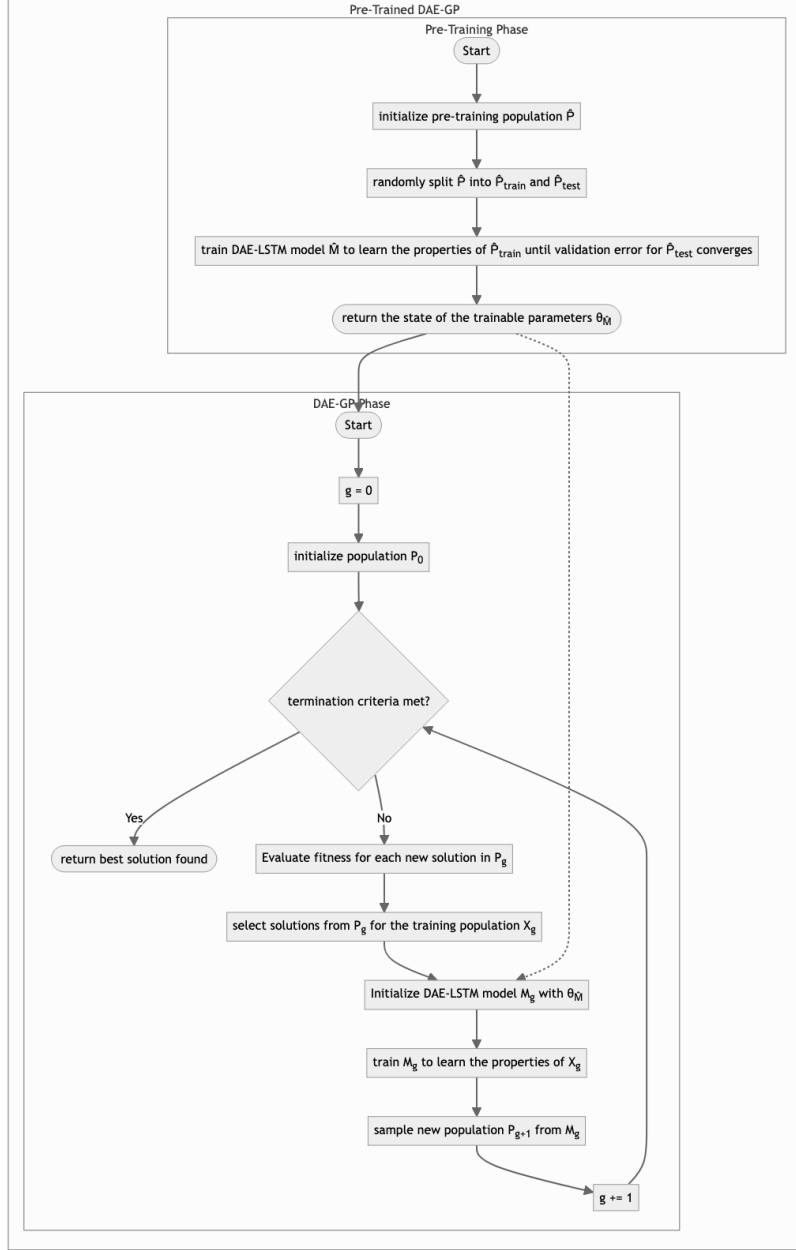


Figure 2: Pre-Trained DAE-GP Flowchart

One difficulty in the implementation of a pre-training strategy into DAE-GP has been the determination of the number of hidden neurons in side the DAE-LSTMs hidden layers. The original description of DAE-GP [33] uses a strategy where the number of hidden neurons for each hidden layer is dynamically set per generation to the maximum individual size inside the current population. For a pre-training implementation, this strategy can not be easily adapted since it leads to a changing number of neurons at each generation resulting in different dimensions of the DAE-LSTM. To allow the sharing of the state of the pre-trained parameters  $\theta_{\hat{M}}$  from the pre-trained model  $\hat{M}$  to each  $M_g$  for  $g \in 1, \dots, g_{\max}$  the number of hidden neurons per hidden layer for all DAE-GP runs, pre-trained as well as regular, is statically set to a predefined value.

If not stated otherwise, all experiments in this thesis use the GP hyperparameters listed in table 1 and the DAE-LSTM specific hyperparameters listed in table 2.

Table 1: GP - Hyperparameter

| Hyperparameter                | Value                          |
|-------------------------------|--------------------------------|
| Population Size               | 500                            |
| Generations                   | 30                             |
| Fitness Metric                | Root Mean Squared Error (RMSE) |
| Train/Test Split              | 50:50                          |
| Maximum Tree Depth            | 17 [14]                        |
| Initialization Algorithm      | Ramped Half and Half [14]      |
| Mix/Max Initialization-Depth  | 2/6                            |
| Selection Operator            | Binary Tournament Selection    |
| Function Set                  | {+ , - , * , AQ [17]}          |
| Ephemeral Constants           | [-5,..,5]                      |
| Pre-Training Population Size  | 10000                          |
| Pre-Training Train/Test Split | 50:50                          |

Table 2: DAE-LSTM - Hyperparameter

| Hyperparameter                              | Value                    |
|---|--------------------------|
| Stopping Condition                          | Convergence [31]         |
| Reconstruction Error Metric                 | Multiclass Cross Entropy |
| Gradient Descent Algorithm                  | Adam Optimization [13]   |
| Learning Rate                               | 0.001                    |
| Batch Size                                  | 0.1                      |
| Sampling Steps                              | 1                        |
| Hidden Layer                                | 2                        |
| Hidden Neurons                              | 150                      |
| Corruption Operator                         | Levenshtein Edit [31]    |
| Denoising Edit Probability (Model Building) | 0.05                     |
| Denoising Edit Probability (Model Sampling) | 0.95                     |
| Pre-Training Stopping Condition             | Early Stopping           |

The framework that was used to run all experiments of this thesis was provided by the supervisor of this thesis David Wittenberg and uses the python programming language [26] in conjunction with the baseline libraries `Keras` [2] for deep neural networks and `deap` [6] for evolutionary computation. For data visualizations I used the python package `matplotlib` [12], statistical analysis and evaluations were conducted using primarily the data science libraries `scipy` [28], `numpy` [8], `pandas` [24], and `IPython` [20].

### 3.2 Benchmark Problem

To test pre-training in DAE-GP this thesis focuses on the domain of real-world symbolic regression problems. Symbolic Regression problems have been one of the first GP applications [14] and are

an actively studied and highly relevant research area. The goal in symbolic regression is to find a mathematical model for a given set of data points [19], in real-world symbolic regression these data points are sourced from real-world observations which in contrast to synthetic symbolic regression problem are more likely to contain random noise and bias. Another important challenge in solving real-world symbolic regression problems is the ability for a given model to generalize, we want the final model to show high accuracy in predicting outcomes for previously unseen cases.

The main experiments conducted in this thesis uses the NASA Airfoil Self-Noise Data Set [1] that consists of 5 input variables and 1 output variable that are listed in table 3.

Table 3: Airfoil - Dataset Description

| Type   | Name | Description                         | Unit          |
|--------|------|-------------------------------------|---------------|
| input  | x1   | Frequency                           | Hertz         |
| input  | x2   | Angle of attack                     | Degree        |
| input  | x3   | Chord length                        | meters        |
| input  | x4   | Free-stream velocity                | meters/second |
| input  | x5   | Suction side displacement thickness | meters        |
| output | y    | Scaled sound pressure level         | decibels      |

The objective of the airfoil problem is to find a function that accurately predicts the output variable  $y$  by taking in a subset of the input variables  $x_1, x_2, x_3, x_4, x_5$ . The function set used by all DAE-GP variations for symbolic regression is summarized in tables 1 and , the terminal set consists of the the input variables  $x_1, x_2, x_3, x_4, x_5$  and the ephemeral integer constants listed in table 1 [32].

## 4 Results for the Airfoil Dataset

### 4.1 Influence on Generalisation

To gather a deeper understanding about the effect of pre-training DAE-LSTM in DAE-GP a series of experiments was conducted using the airfoil dataset for symbolic regression while using different parameter configurations for the number of hidden layers as well as the number of hidden neurons per hidden layer.

To study generalization behavior this series of experiments is conducted using DAE-GP with only a single generation until the search terminates. I disregard the fitness of solutions found and focus solely on the reconstruction error that is produced during the training of each DAE-LSTM. The reconstruction error is measured for two separate populations, a training population  $P_{train}$  that is used to train our DAE-LSTM as well as a hold-out validation population  $P_{test}$ . For the pre-trained DAE-GP two additional, separate populations  $\hat{P}_{train}$  and  $\hat{P}_{test}$  are used exclusively for pre-training.

DAE-GP is tested in two different configurations:

- Variable number of hidden neurons (50, 100, 200) with a single hidden layer
- Fixed number of hidden neurons (100) per hidden layer with variable number of hidden layers (1, 2, 3)

For each configuration I tested traditional DAE-GP as well as a pre-trained DAE-GP resulting in 12 total sub experiments that were each based on 10 individual runs (total number of runs=120). To avoid creating biased results through the presence of sampling error inside the pre-training

population (see [23]), the population size for the pre-training phase is chosen very high with the size of  $\hat{P} = 10000$  where 50% of  $\hat{P}$  is used for the training population  $\hat{P}_{train}$  and the remaining 50% are used for the hold-out validation population  $\hat{P}_{test}$ . The training of DAE-LSTM uses a fixed number of 1000 epochs until termination and uses Adam optimization for gradient descent. The reason for using a high amount of 1000 fixed training epochs is to deliberately force the DAE-LSTM to overfit to the training data.

In general I expect that with a growing number of trainable parameters (either by adding more hidden layers or more hidden neurons per layer) the DAE-LSTM will be more prone to overfit to the training population  $P_{train}$  resulting in a small reconstruction error for the training population and a large one for the validation population  $P_{test}$ . The reason for this effect is that a larger network trained over an extended period of time (without the use of strategies like early stopping), has much more potential to learn noise from the training dataset than a smaller network, which is more likely to result in worsening performance for previously unseen cases [29].

Based on the review of [5] I also expect that pre-training will have an insignificant or even negative influence on small DAE-LSTM instances while improving the networks generalization ability with growing size.

Figure 3 summarizes the median reconstruction error for a variable number of hidden neurons. As expected, increasing the number of hidden neurons leads to stronger overfitting to the training dataset which results in small training errors but growing testing errors. For the experiments run with 50 and 100 hidden neurons, a small benefit of using pre-training can be observed. Using only 50 hidden neurons leads to a smaller gap between training and testing error for the pre-trained DAE-LSTM. For 100 hidden neurons, regular DAE-GP not only starts to overfit to the training data earlier than pre-trained DAE-GP, also it can be seen that pre-trained DAE-GP starts to overfit at a lower reconstruction error which would result in a higher model performance if training strategies such as early stopping would be employed. Doubling the number of hidden neurons to 200 results in very strong overfitting behavior for both DAE-GP variants starting around the 200.th epoch.

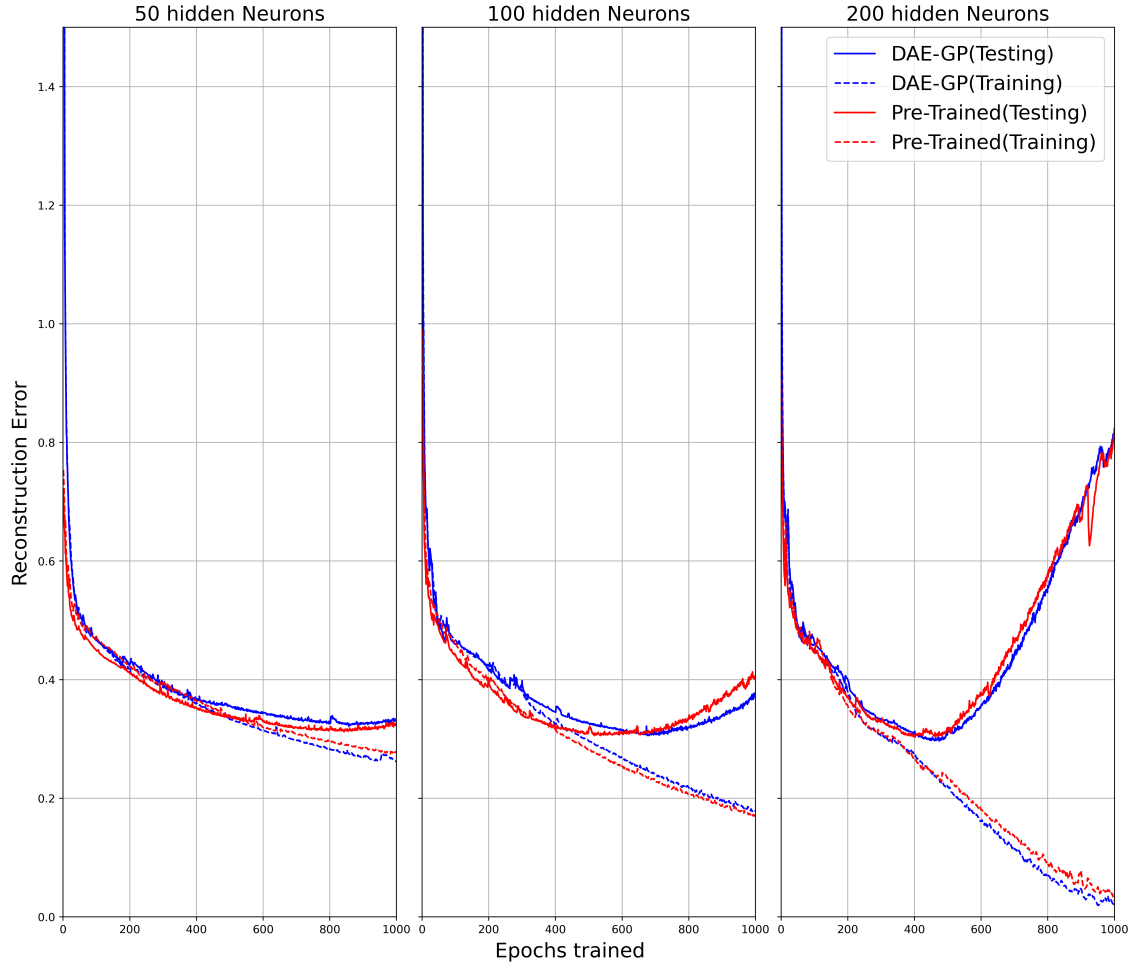


Figure 3: First Generation Median Reconstruction Error for variable number of hidden Neurons

The results for the experiment with varying number of hidden layers are summarized in figure 4. Again, it can be observed that by increasing the dimension of the DAE-LSTM network both algorithms increasingly overfit to the training data. While for a single hidden layer overfitting begins at around the 400th. epoch, doubling the number of hidden layers to two leads to both algorithms overfitting at around the 200.th epoch. In general over all three sub experiments, both algorithms start to overfit after approximately the same number of epochs but pre-training leads to reaching the point of overfitting at a higher reconstruction error which would result in a inferior model performance if the early stopping training strategy would be used during model training.

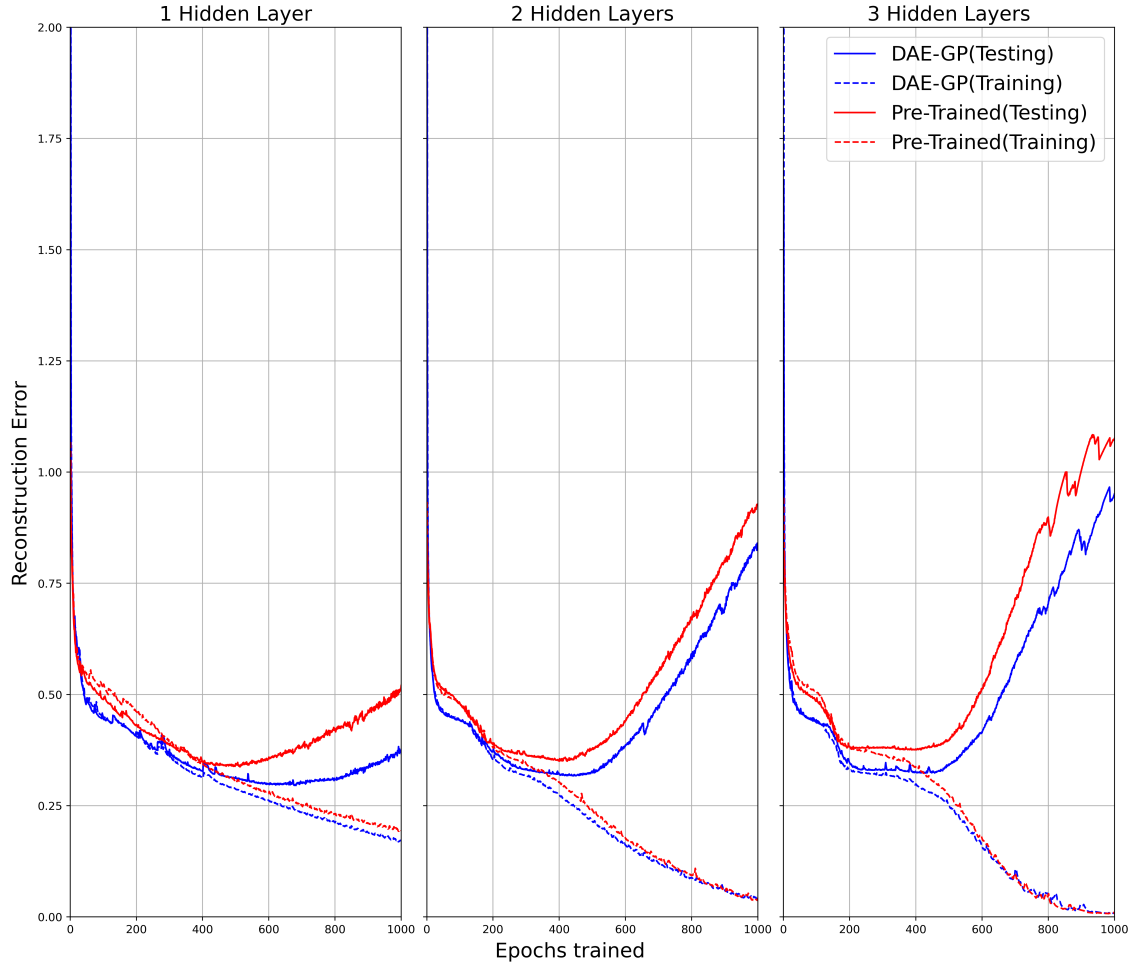


Figure 4: First Generation Median Reconstruction Error for variable number of hidden Layers

## 4.2 Influence on solution quality

After closely examining the effect of pre-training on DAE-GPs generalization behavior another series of experiments is conducted to study how pre-training influences the overall search behavior of DAE-GP. The airfoil problem was selected as a first benchmark problem to test pre-trained DAE-GP against traditional DAE-GP.

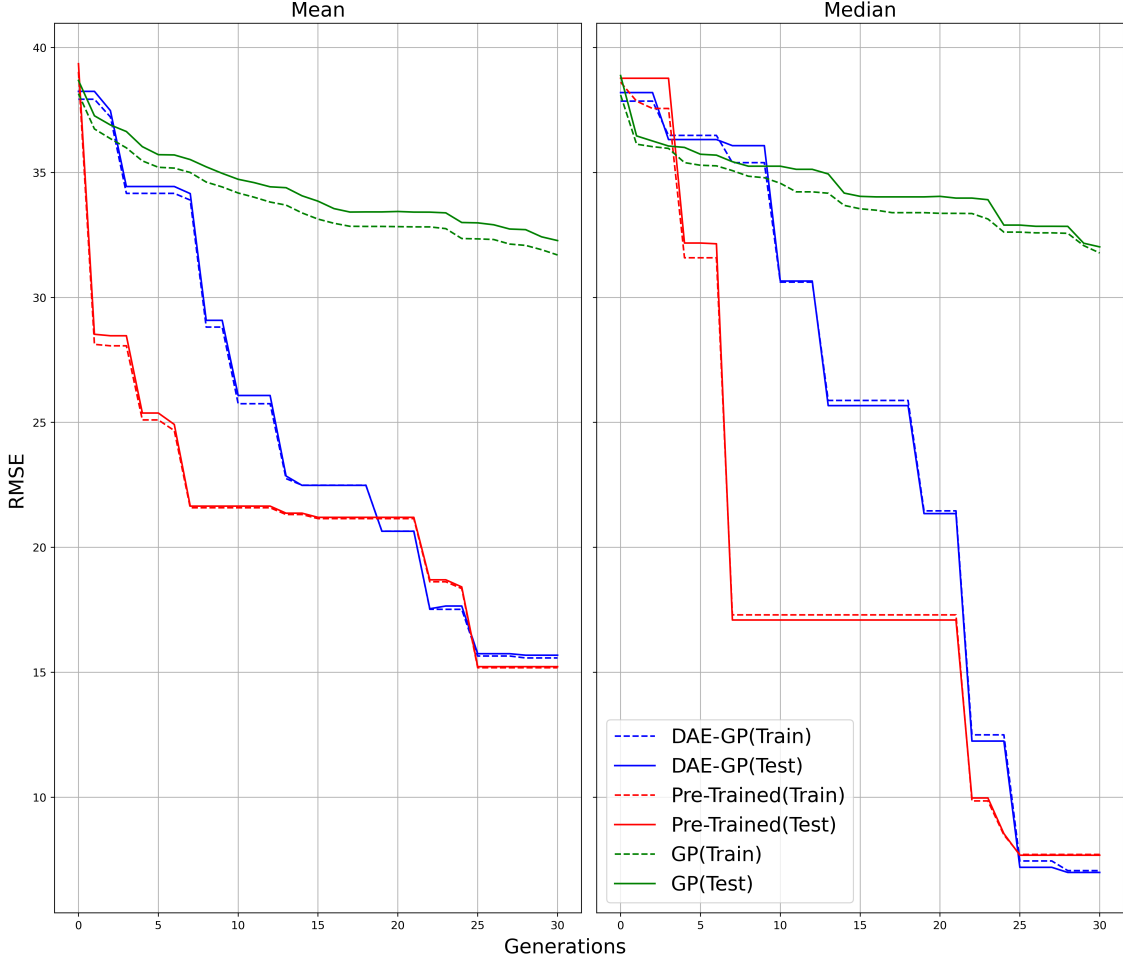


Figure 5: Best Fitness over 30 Generations - Airfoil

Figure 5 shows both the mean and median of the best fitness for each generation on both the test and training set of the airfoil dataset for using 2 hidden layers inside the DAE-LSTM networks. The results are aggregated for 10 individuals runs per algorithm and also include regular GP as a benchmark. For all three algorithms an improvement in the best found fitness can be observed during the evolutionary search but the results show that DAE-GP based algorithms, on average, find solutions with much higher fitness as traditional GP.

The first interesting observation from this experiment is, that the pre-trained DAE-GP shows slightly lower mean RMSE (higher fitness) but a higher median RMSE (lower fitness) than regular DAE-GP for both the training and the testing set in overall fitness. Regarding the presence of overfitting, both DAE-GP variants show only a very small gap between the testing and training fitness which indicates a good generalization behavior. Another interesting observation from figure 5 is that pre-trained DAE-GP is faster at improving fitness than regular DAE-GP, this is especially true if only looking at the first 10 generations. The median best RMSE on the test set after 10 generations for pre-trained DAE-GP is 17.093 which is smaller by a factor of 0.558 than regular DAE-GP with a median best RMSE of 30.658

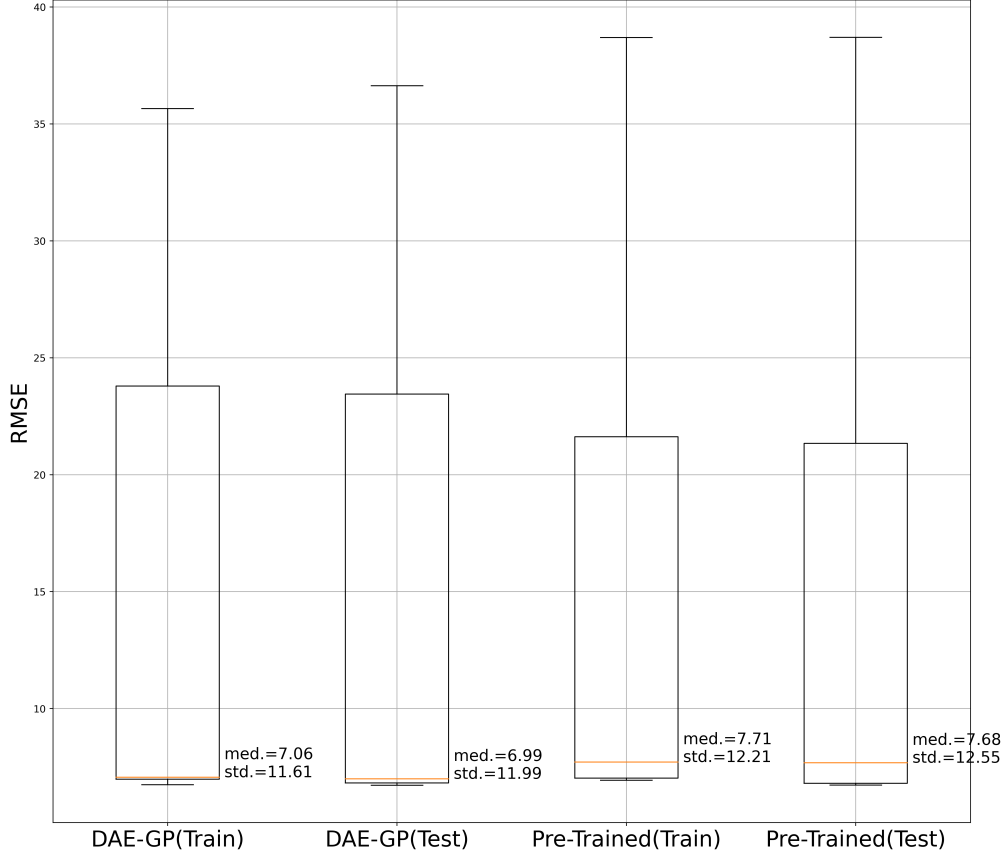


Figure 6: Best Fitness after 30 Generations - Airfoil

The distribution of final fitness scores for pre-trained and regular DAE-GP are visualized as box plots in figure 6. The distribution for regular DAE-GP shows to be preferable to that of pre-trained DAE-GP since it has a lower median RMSE of 6.991 for the test set (7.68 for pre-trained DAE-GP) as well as less dispersion of the solutions measured by a standard deviation of 11.989 (12.548 for pre-trained DAE-GP). For reference, the median final RMSE for the test set of standard GP is at 32.024 which is larger by a factor of 4.17 if compared to pre-trained DAE-GP.

An interesting observation from studying the distribution of final fitness scores for both algorithms is that pre-trained DAE-GP has a smaller interquartile range and more extreme outliers for high RMSE which explains the slightly worse performance if looking at median best fitness present in figure 5.

Since previous work by [32] demonstrated that DAE-GP, for a given number of 10.000 fitness evaluations, is able to produce solutions that are much smaller in tree size than regular GP, I also studied the influence of pre-training on the size of solutions found by DAE-GP. Figure 7 shows the median of both the average size of individuals inside the population as well as the size of the currently best performing solution inside the population. It can be observed that both DAE-GP variants strongly reduce the average solutions size already in the first generations and that the average solution size inside the population constantly stays at this very low level for the rest of the search. The median average size over all generations is 1.536 for DAE-GP and 1.536 for pre-trained DAE-GP. Regarding the size of the best solution per generation, the results show that the pre-trained version of algorithm did produce solutions with the same median size as traditional DAE-GP. The

median size of the best solutions found after terminating the search is the same for both algorithms (DAE-GP: 5, Pre-Trained DAE-GP: 5)

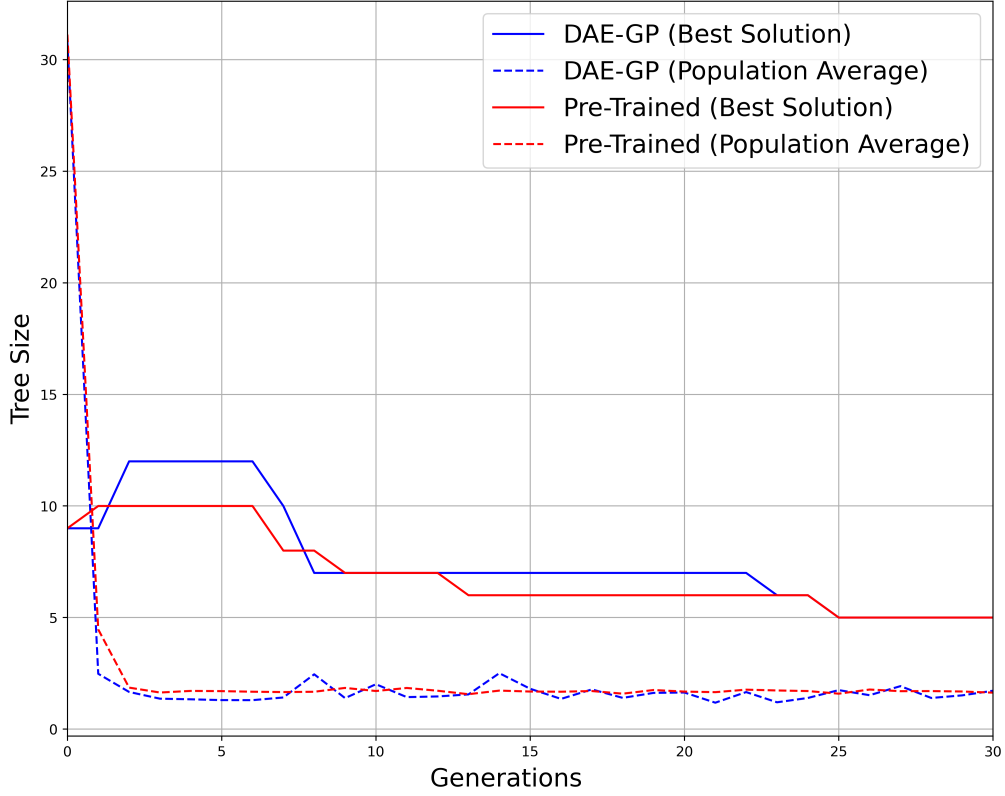


Figure 7: Median Solution Size over 30 Generations - Airfoil

Another interesting metric to examine in population-based optimization algorithms is the diversity of the current generations population. Since individual solutions in DAE-GP are computer programs in the form of parse trees, I selected the normalized Levenshtein edit distance [15] as my primary metric for tracking population diversity. Figure 8 shows the median population diversity for both DAE-GP algorithms and regular GP as a benchmark. While the population diversity steadily decreases over the generations for standard GP, DAE-GP variants strongly increase the population diversity in the first generations and keep them at a higher level during the evolutionary search. Here it can be observed, that pre-training shows a positive effect by increasing population diversity in comparison to regular DAE-GP (Median over all generations for DAE-GP: 0.861, Pre-Trained DAE-GP: 0.925, Standard-GP 0.705)

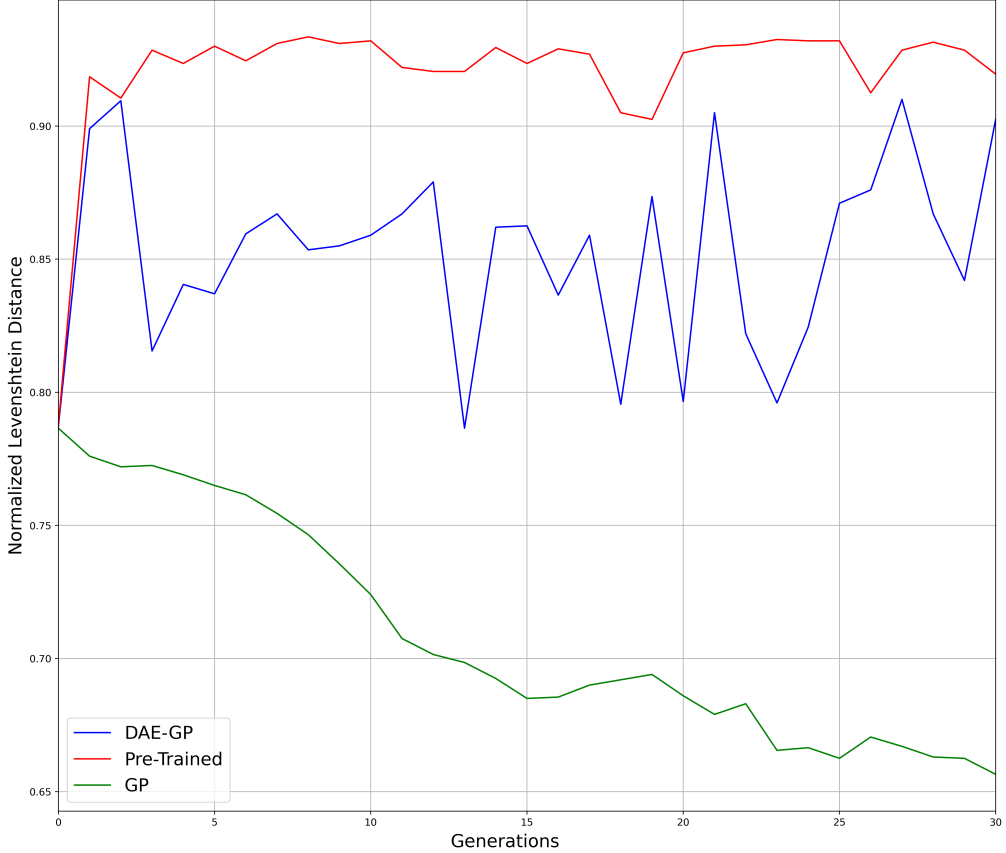


Figure 8: Median Population Diversity over 30 Generations - Airfoil

#### 4.2.1 Dynamic Adjustment of Hidden Neurons

To ensure a fair comparison between pre-trained and regular DAE-GP, the prior experiments used a static number of hidden neurons for each hidden Layer inside the DAE-LSTM networks. For comparison, figure 9 shows the total number of trainable parameters for each generation’s DAE-LSTM of another experiment where regular DAE-GP was tested with dynamic adjustment of the number of hidden neurons as described in [33] and [32]. Again, the experiments was based on 10 individual runs and otherwise used the same hyperparameters as listed in tables 1 and 2. It clearly shows that DAE-GP can strongly reduce the number of trainable parameters by adjusting the number of hidden neurons per hidden layers to the current generations population which largely reduces the amount of training necessary and likely reduce the run-time of DAE-GP.

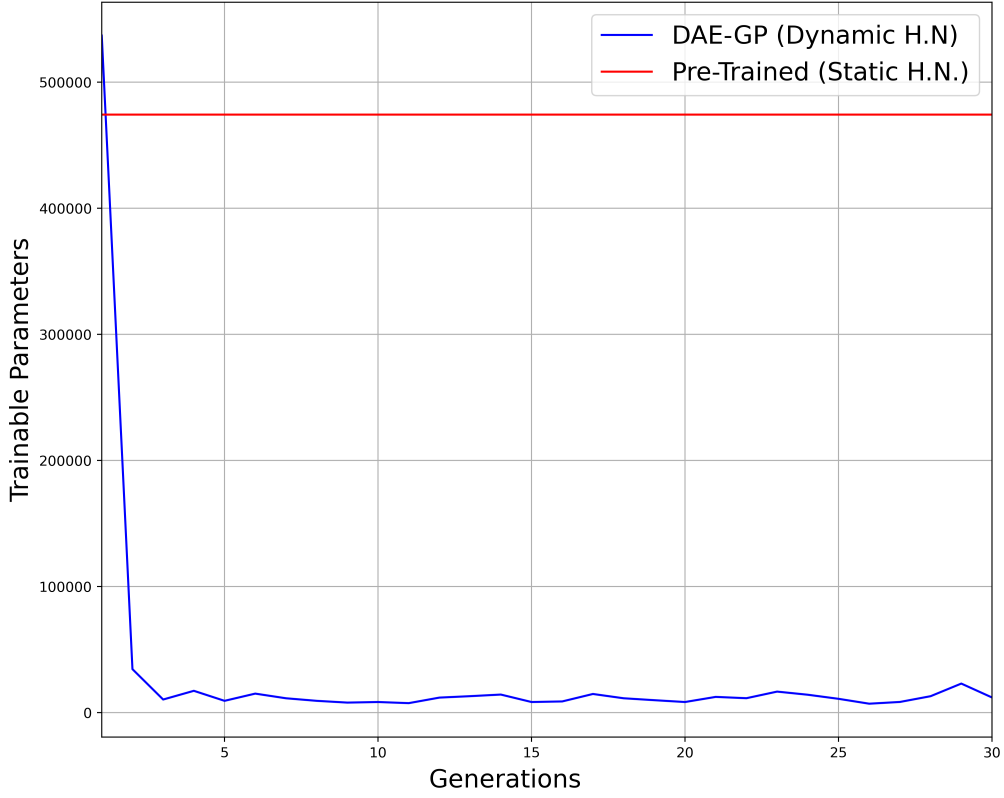


Figure 9: Median Number of trainable Parameters over 30 Generations - Airfoil - Dynamic adjustment of regular DAE-GP

As expected, this reduction of hidden neurons by dynamic adjustment, does also result in a reduction of the fitness of solutions found. Figure 10 shows that pre-trained DAE-GP, with it's more complex DAE-LSTMs over the full 30 generations, does achieve a higher median fitness than regular DAE-GP with dynamic adjustment of hidden neurons. Pre-Training does therefore introduce a new Trade-Off decision into the adjustment of DAE-GP hyperparameters where the number of hidden neurons needs to be carefully selected since it positively impacts solution quality but also increases the computational cost of DAE-LSTM training.

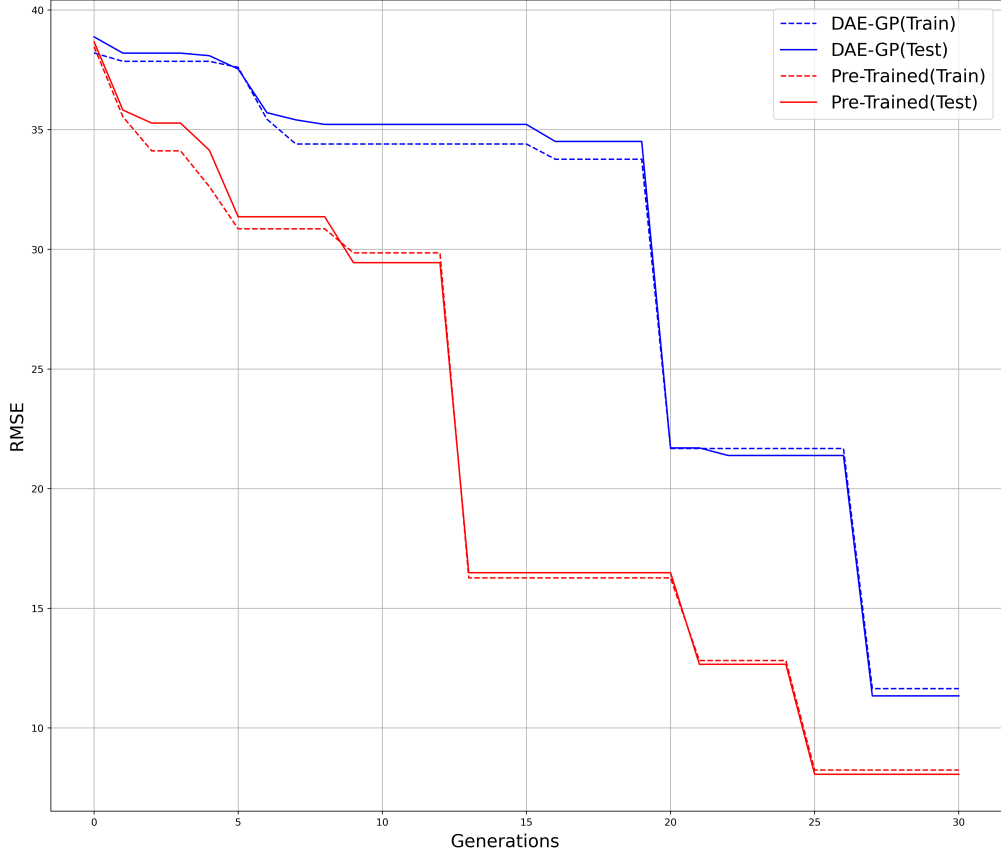


Figure 10: Median Best Fitness over 30 Generations - Airfoil - Dynamic adjustment of regular DAE-GP

#### 4.2.2 Reduced Number of Hidden Layers

Since previous research on DAE-GP used a single hidden layers for the airfoil dataset [32], I repeated the experiment with a single hidden layer. Based on the findings of [5], I expected that pre-training DAE-GP would lead to a decrease in overall performance. Figures 11 and 12 shows the mean and median best fitness per generation as well as the distribution of final fitness scores after 30 generations. The results are, again, based on 10 individual runs per algorithm. As expected the results show, that for a small DAE-LSTM size pre-training negatively impacts the fitness of solution found by DAE-GP. The median final RMSE for the test set of pre-trained DAE-GP increases by a factor of 1.287 to 16.213 compared to regular DAE-GP with 12.594.

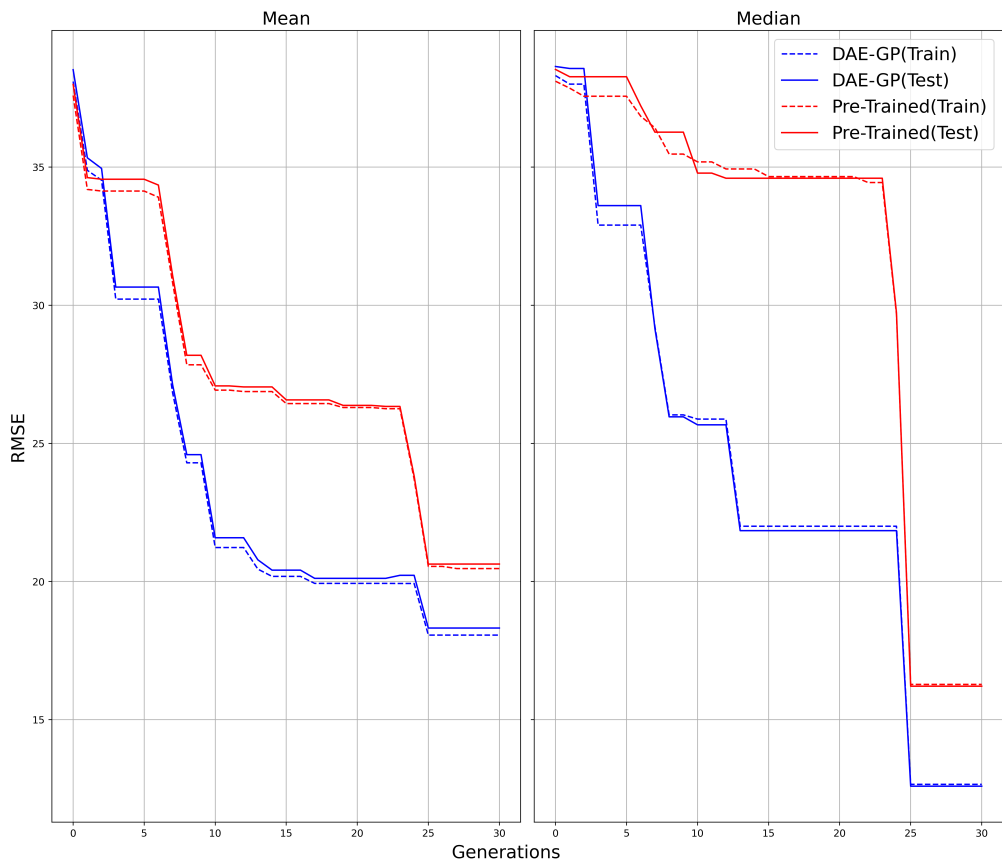


Figure 11: Fitness over 30 Generations - Airfoil - Single Hidden Layer

Interestingly, figure 12 shows that the distribution of final fitness scores for pre-trained DAE-GP has a larger interquartile range than regular DAE-GP. This is opposed to the distributions of final fitness score that was measured for the same problem run with two hidden layers (see figure 6). Otherwise, pre-trained DAE-GP again has more outliers for high RMSE than regular DAE-GP as seen in the previous experiment with 2 hidden layers.

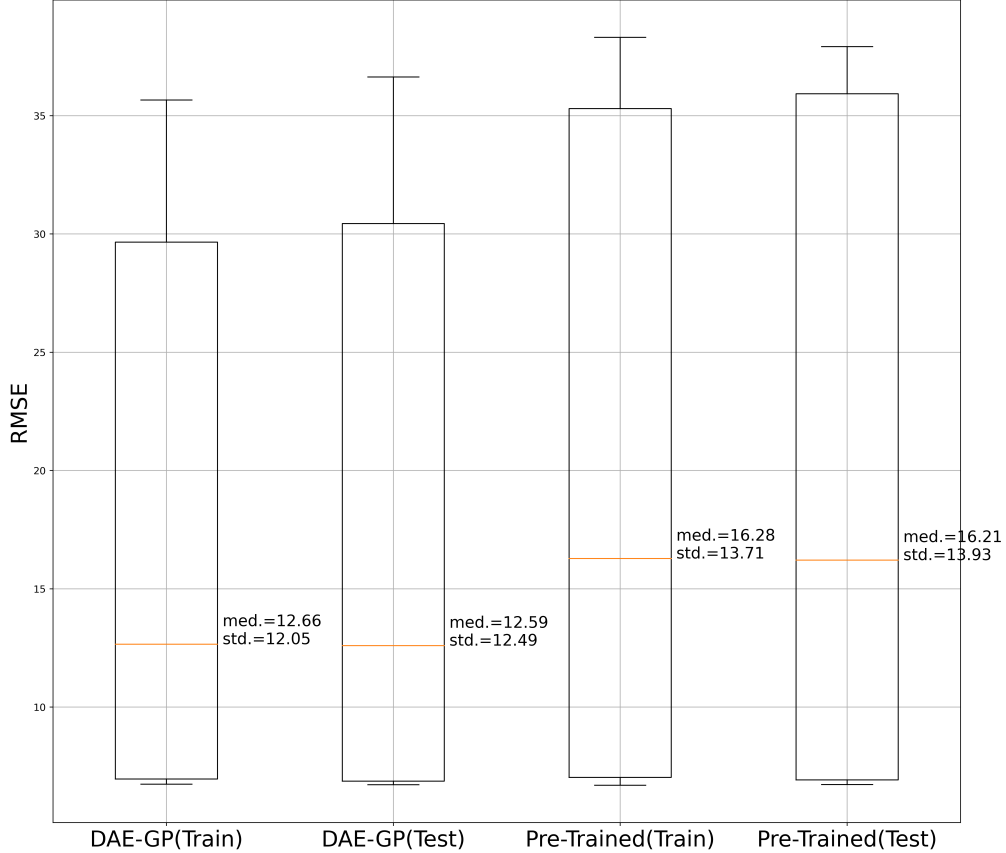


Figure 12: Fitness after 30 Generations - Airfoil - Single Hidden Layer

#### 4.2.3 Alternative Pre-Training Strategies

Since pre-training thus far did not demonstrate significant benefits for the quality of solutions found by DAE-GP, this section describes two alternative pre-training strategies, Second Generation Pre-Training and Grow-Initialized Pre-Training, that are also tested for the airfoil dataset.

One common observation in GP-based optimization algorithms is that the largest improvements in fitness are often occurring in the first generation of the search process. Second Generation Pre-Training tries to exploit this observation by shifting the pre-training phase from the start of the algorithm into the second generation with the aim to produce a pre-training Population  $\hat{P}$  that more accurately captures the properties of the search problem. The basic idea is to run regular DAE-GP for the first generation without any interference, after completing the first generation, the pre-training population  $\hat{P}$  is created by sampling the DAE-LSTM model  $M_1$ . The pre-training model  $\hat{M}$  is then trained using  $\hat{P}$ , after finishing DAE-GP continues running and initializes each new DAE-LSTM model  $M_g$  for  $g \in 2, \dots, g_{max}$  using the trainable parameters  $\theta_{\hat{M}}$ .

The pre-training implementation in previous experiments used ramped half and half initialization [14] to create  $\hat{P}$ , this leads to 50% of the population consisting of full grown trees. An alternative method of initializing  $\hat{P}$  is to use the grow initialization method where solutions are not guaranteed to be full trees. This different structural composition of solutions inside the pre-training population might be another way to improve the pre-training strategy by training on a population that more closely resembles the structural properties of further generations population where a lower percentage

of full grown trees is to be expected.

Figure 13 shows the median best fitness by generations for both alternative pre-training strategies as well as the results for standard DAE-GP and the standard Pre-Training implementation used in earlier experiments. Unfortunately, both alternative strategies do show a worse performance in fitness than both DAE-GP and standard pre-trained DAE-GP resulting in lower fitness.

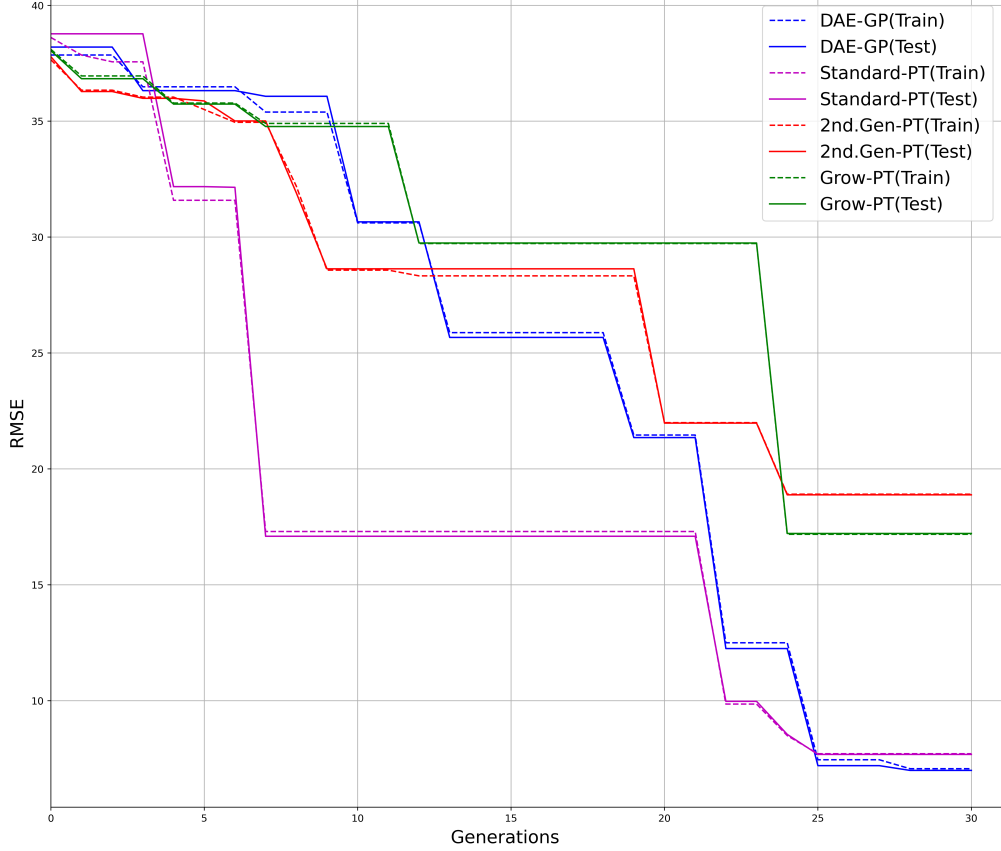


Figure 13: Best Fitness over 30 Generations - Airfoil - Alternative Pre-Training Strategies

Figure 14 shows the distribution of best fitness achieved on the test set after running for 30 full generations. Both alternative second generation Pre-Training as well as grow-initialized Pre-Training show a much higher median RMSE (18.88/17.21) compared to standard pre-training (8.55) and regular DAE-GP (6.99). Also both approaches do not demonstrate any benefit on the dispersion of solutions found resulting in similar standard deviations if compared to standard pre-training.

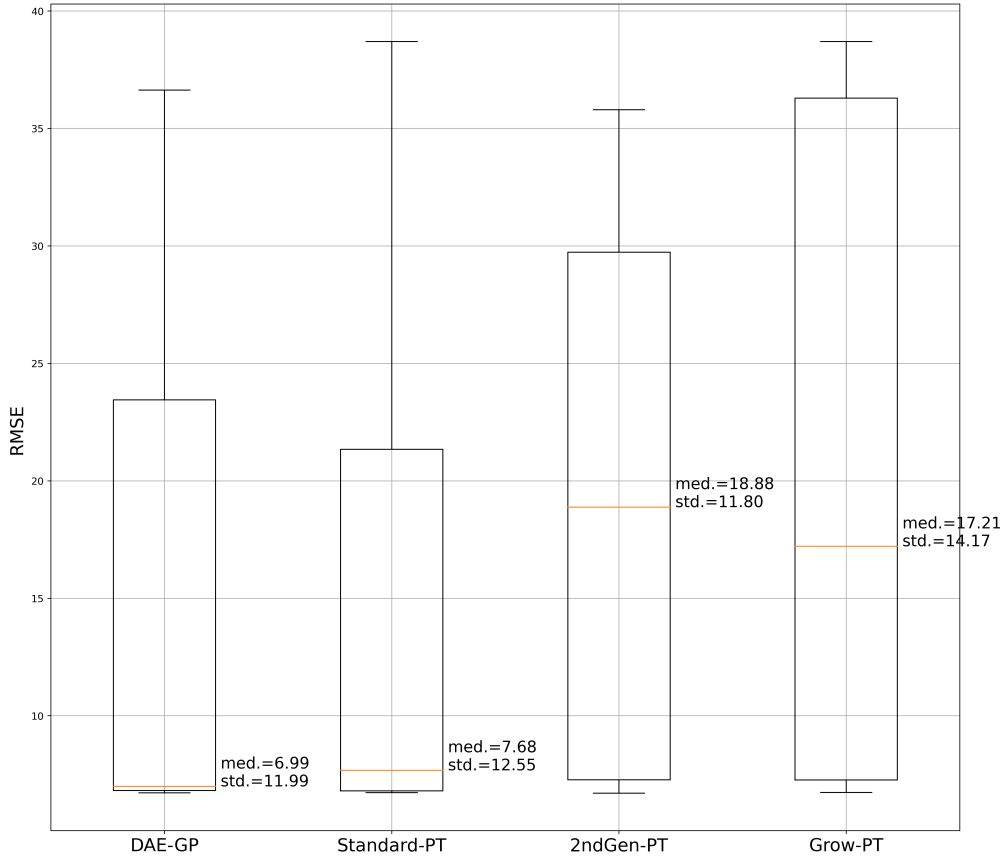


Figure 14: Best Fitness on Test Set after 30 Generations - Airfoil - Alternative Pre-Training Strategies

### 4.3 Influence on Run-Time

One important argument for using pre-training with DAE-GP is that it might be a potential way to reduce the overall run-time of the algorithm by reducing the training time of each generation’s DAE-LSTM model. Especially in the context of optimization problems where solutions have to be found numerous times in a time efficient manner (e.g. Vehicle Routing in the Domain of Logistic Services), one major advantage of pre-training is that a pre-trained model can be re-used to optimize many instances of an optimization problem.

The run-time analysis in this chapter is based on experiments that were all executed on an Intel® Xeon® W-2245 Processor without the use of graphical processing unit (GPU) acceleration in the training of DAE-LSTM networks. Since the framework that was used is written in the, comparatively slow, python programming language, the absolute run-time measurements are only of limited meaningfulness. Nonetheless, by analyzing the relative run-time differences between DAE-GP and its pre-trained alternative, the influence of pre-training on DAE-GP run-time can be explored.

Surprisingly, as shown in figure 15, for the experiment conducted on the airfoil dataset with 2 hidden layers a strong negative impact of pre-training can be observed for the median run-time of DAE-GP. If the time spend on pre-training is included into the total run-time, the median duration for pre-trained DAE-GP over all 10 runs increases by a factor of 3.121 from a median run-time of

4712.303 seconds for regular DAE-GP to 14706.47 seconds for the pre-trained algorithm. Even in the case where the time spend for pre-training is excluded from the total run-time, pre-training still increases the run-time of DAE-GP by a factor of 2.66 to 12536.89 seconds.

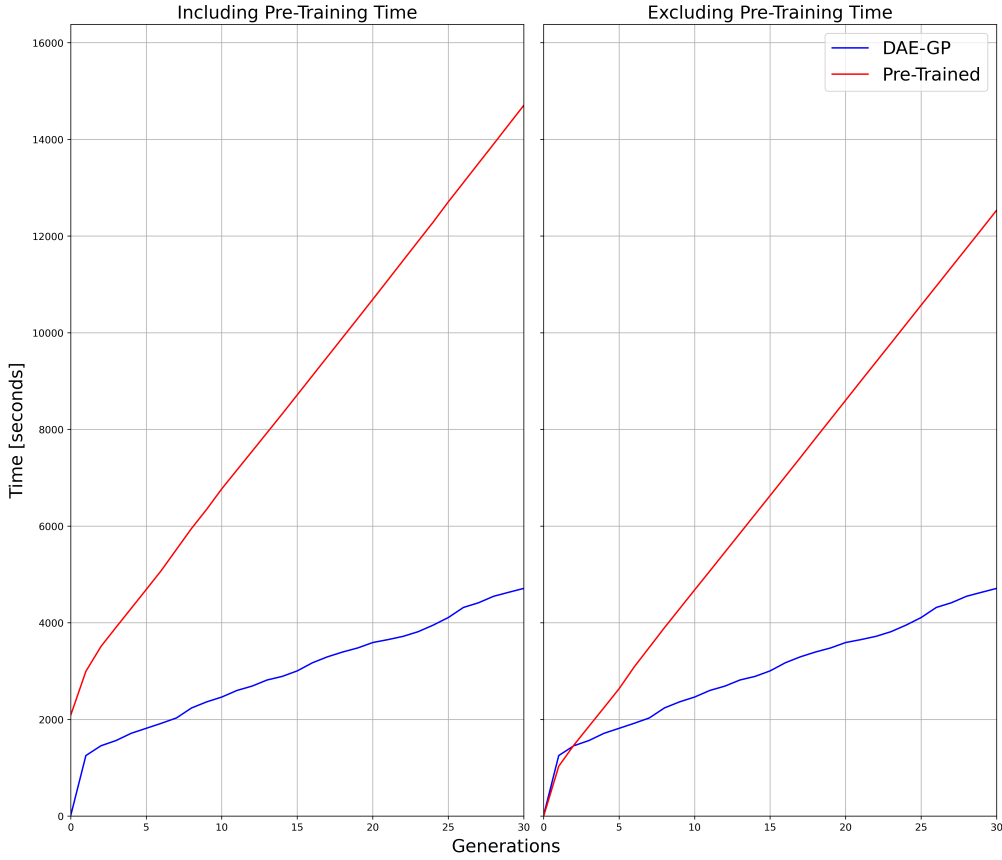


Figure 15: Median Runtime - Airfoil

Figure 16 shows the distribution of the total runtime for both DAE-GP variants. It shows that Pre-Training, besides largely increasing the median runtime, also leads to a higher dispersion which is shown by both a larger interquartile range as well as by a standard deviation that increases by a factor of 1.232 from 635,04 for regular DAE-GP to 782,68 for pre-trained DAE-GP.

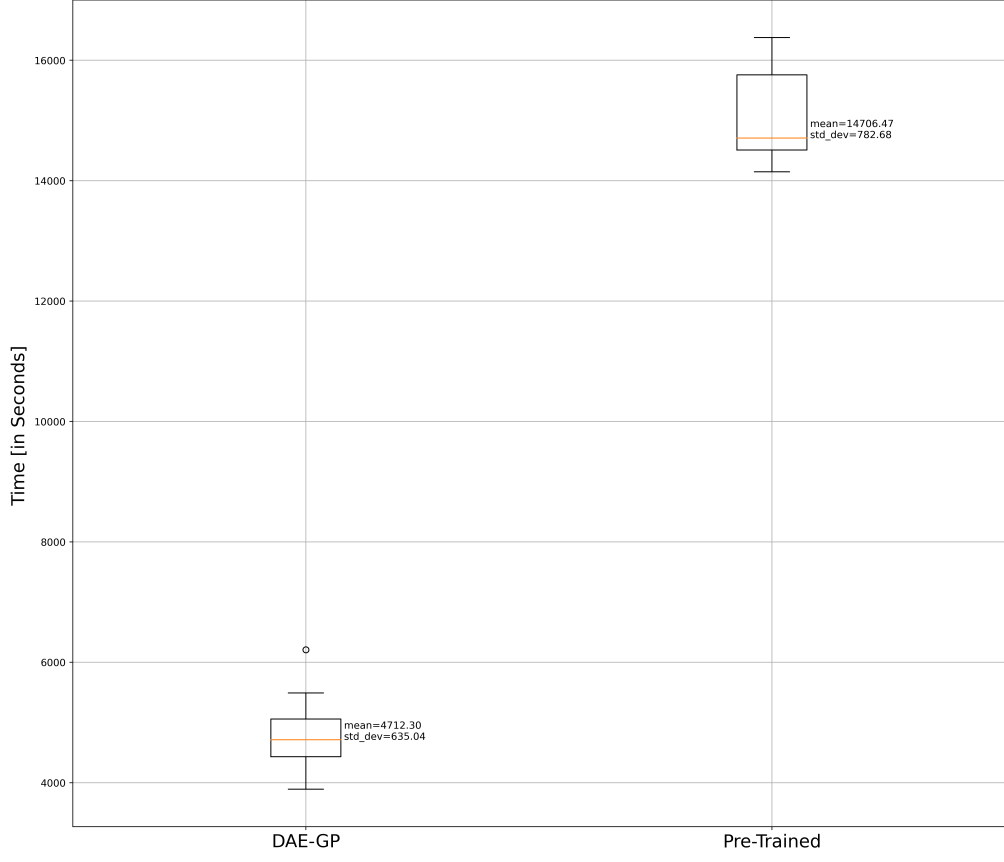


Figure 16: Total Runtime Boxplot - Airfoil

To investigate the strong negative impact of pre-training on DAE-GP run-time, I first studied the influence of pre-training on the median number of training epochs that had to be spent at each generation for the training of the DAE-LSTM models  $M_g$  (excluding the pre-training DAE-LSTM model  $\hat{M}$ ). Figure 17 shows that pre-training, as expected, strongly reduces the number of training epochs that had to be executed at each generation until the termination condition was reached. While regular DAE-GP trains for a median of 122 epochs at each generation, pre-training reduces the number of median training epochs by a factor of 0.439 to 53.5 training epochs.

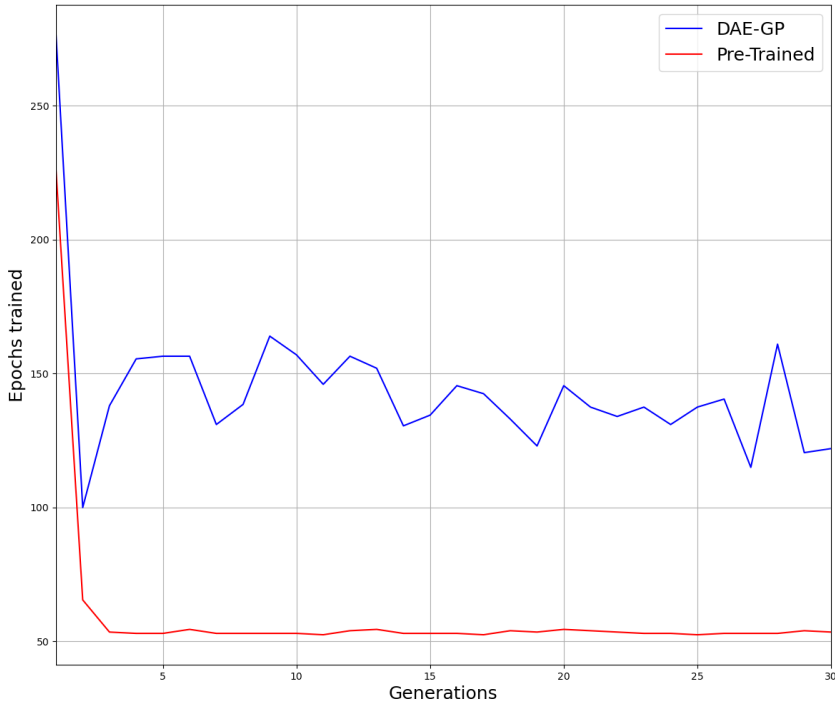


Figure 17: Median Number of Training Epochs per Generation - Airfoil

If we look at another time consuming operation in DAE-GP, the creation of new individuals by sampling the DAE-LSTM model  $M_G$ , we see one main reason for the large run-time increase by pre-training DAE-GP. Figure 18 shows the median sampling time spend during each generation of the search and it clearly demonstrates that pre-training does strongly increase the time spent on model sampling in comparison to regular DAE-GP. The median time spend on sampling new individual for regular DAE-GP increases by a factor of 6.83 from 29.05581 seconds to 198.4503 seconds.

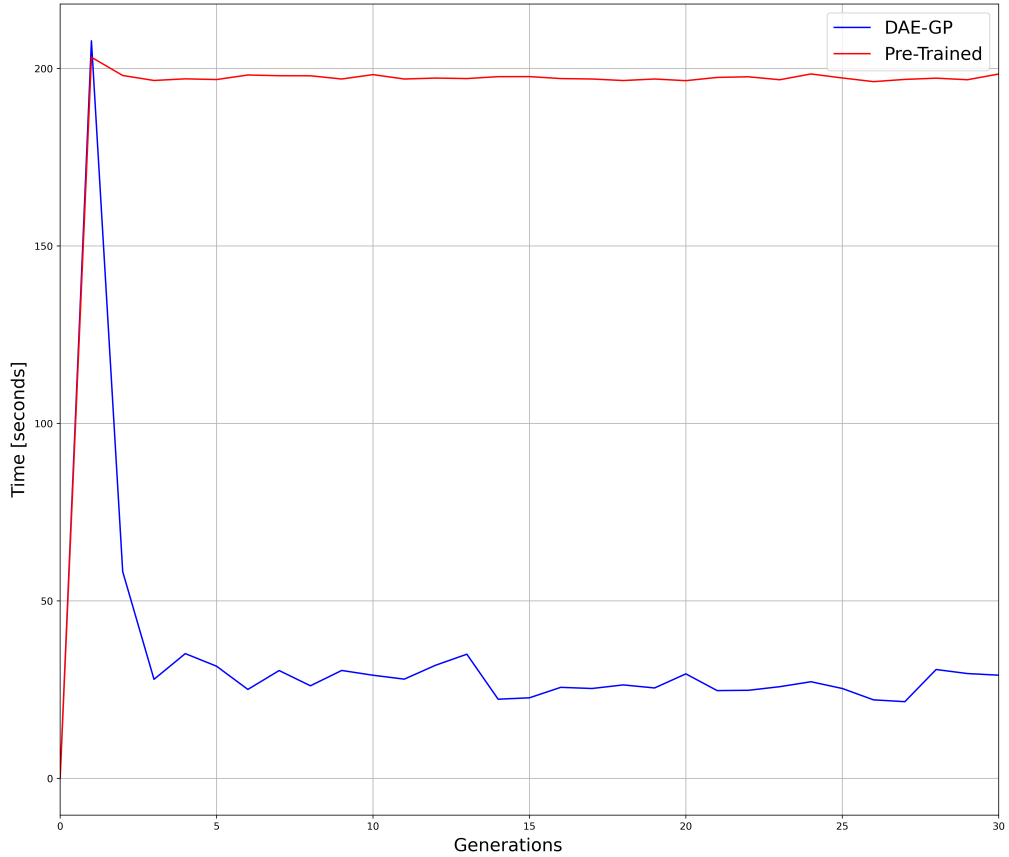


Figure 18: Median Sampling Time per Generation - Airfoil

Surprisingly, even after correcting the run-time for both DAE-GP results by removing the time spent during sampling, my implementation of pre-training for DAE-GP still on average takes more time to finish the search process as shown in figure 19. While traditional DAE-GP has a median run-time without sampling time of 3550.277 seconds , the run-time of pre-trained DAE-GP, without time for sampling and pre-training, still increases by a factor of 1.865 to 6622.027 seconds.

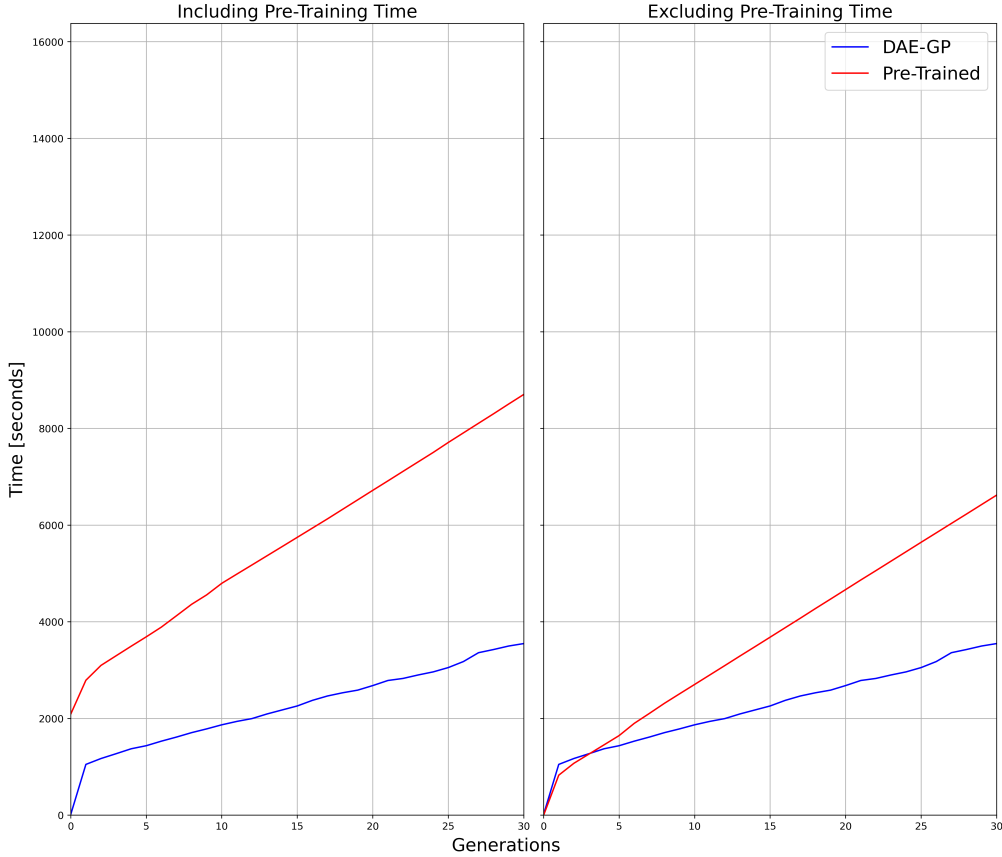


Figure 19: Median Runtime excluding Time for Sampling - Airfoil

While investigating other reasons for the differences in run-time, I verified that both DAE-GP variants use the exact same number of trainable parameters for each generations DAE-LSTMS models (total number of trainable parameters DAE-GP=573473, Pre-trained DAE-GP=573473). After profiling a single run of DAE-GP and pre-trained DAE-GP using the python `cProfiler` module, my best explanation for the remaining differences in run-time is an inefficiency in my implementation of pre-training. Figure 20 shows the cumulative time spend for the 20 most expensive function calls. Even though it is difficult to identify the exact reasons for the performance hit for pre-trained DAE-GP, it shows two interesting findings: Firstly, both algorithms spend relatively more time during model sampling (calls to `DAE_LSTM.py:208(sample)`) than during model training (calls to `training.py:1303(fit)`). Secondly, it shows that internal error handling of the baseline neural network library `keras` (calls to `traceback_utils.py:138(error_handler)` and `traceback_utils.py:59(error_handler)`) takes up a comparatively larger amount of run time for pre-trained DAE-GP than for regular DAE-GP.

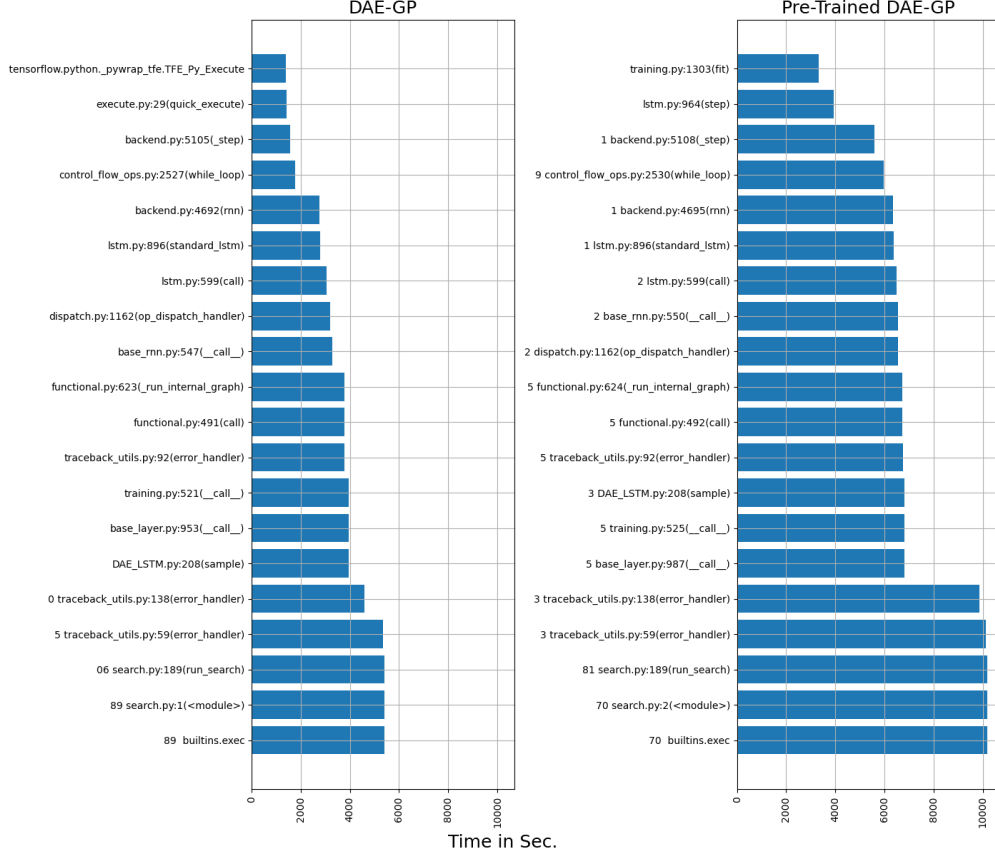


Figure 20: Cumulative Time consumption by Function Calls (Top 20) - Airfoil

## 5 Results over different Real-World Symbolic Regression Problems

To gather more confidence in the previous results, I applied the pre-training strategy for DAE-GP to three additional real world symbolic regression problems. Table 4 briefly summarizes the benchmark problems.

Table 4: Real World Symbolic Regression Benchmark Problems

| Problem        | Observations | Features | Source |
|----------------|--------------|----------|--------|
| Airfoil        | 1503         | 5        | [1]    |
| Boston_Housing | 506          | 13       | [9]    |
| Energy_Cooling | 768          | 8        | [25]   |
| Concrete       | 1030         | 8        | [34]   |

To test for statistical differences of the results achieved by either pre-trained or regular DAE-GP, I selected the nonparametric Mann-Whitney-U Test ([30], [16]) to test for differences in the distribution underlying the samples sourced from my experiments. Additionally, I included the effect strength of pre-training as measured by Cliffs Delta [3] into the statistical analysis. Better median values

(e.g. higher fitness) are printed bold and p-values are marked with asterisk (**1,2,3**) for  $\alpha$  levels (0.1, 0.05, 0.01).

Note that the results for the real world symbolic regression problems inside this chapter, except for the airfoil problem (see subsection [Influence on Run-Time](#)), have not been analyzed for their total run-time. This is due to the fact, that experiments were run on different computers architectures which resulted in strongly biased results.

## 5.1 Influence on Fitness

The results for the median best fitness over the evolutionary search are visualized in figure 21. Figure 22 shows the distribution of final fitness values on both the test and training set as box plots.

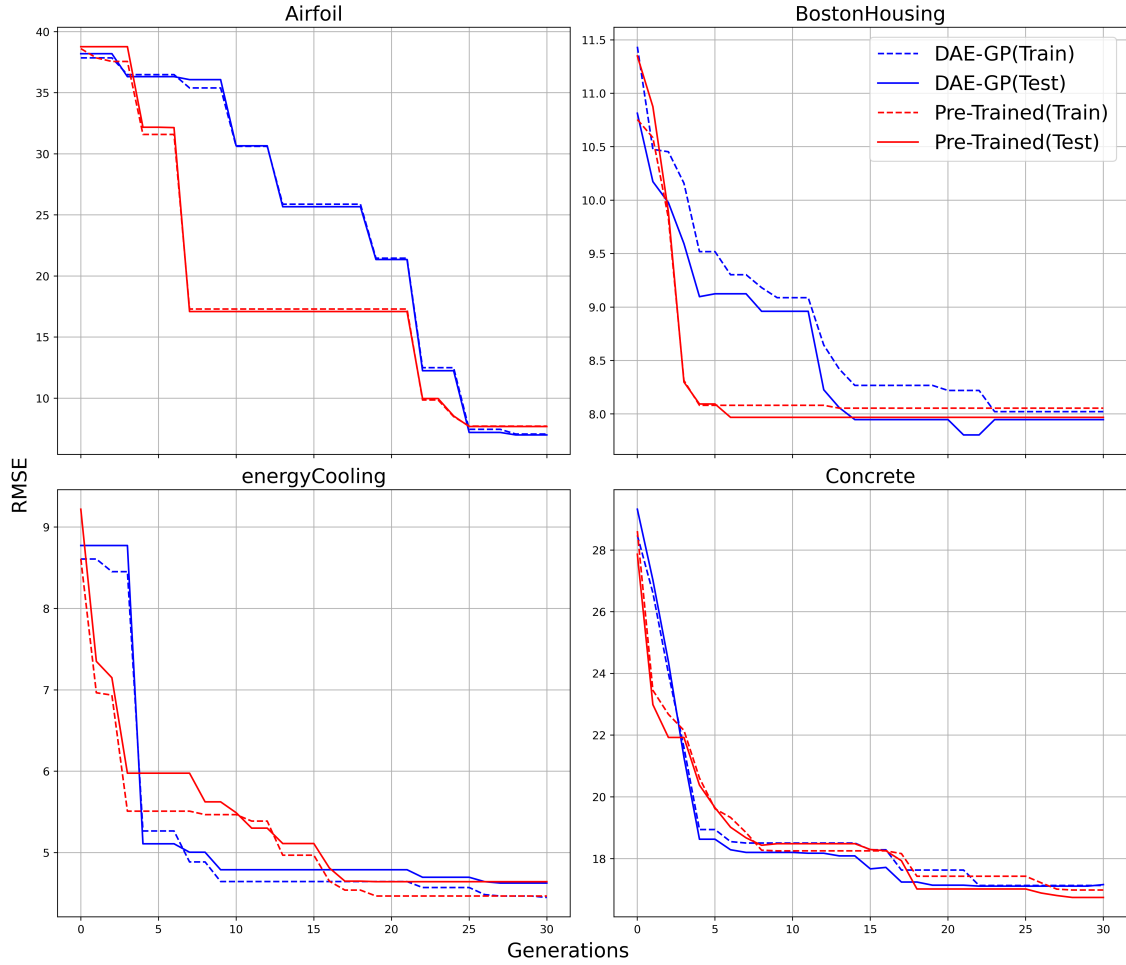


Figure 21: Fitness over 30 Generations - Real World Symbolic Regression

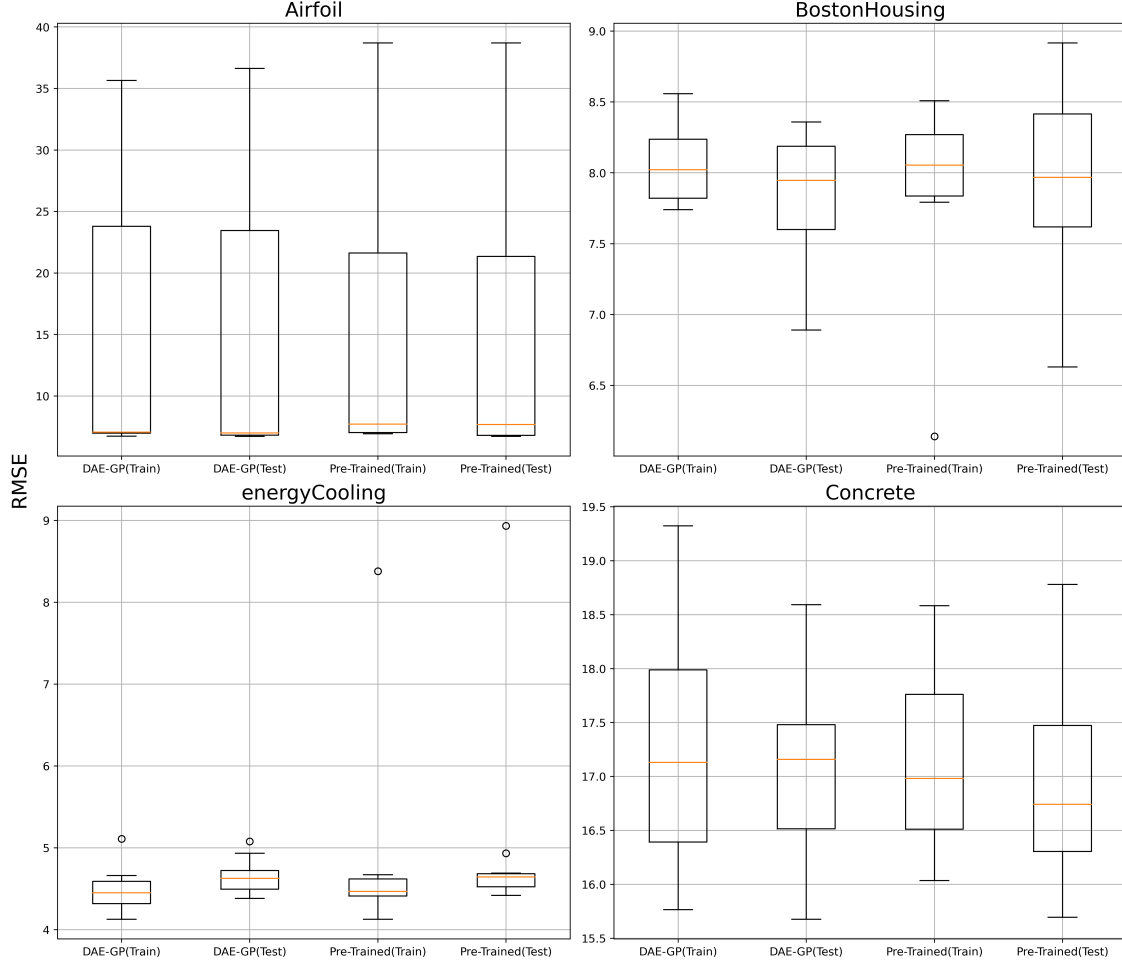


Figure 22: Fitness after 30 Generations - Real World Symbolic Regression

Table 5 summarizes the results for the median best fitness achieved after 30 generations and shows the results of computing the statistical tests.

Table 5: Median Best Fitness after 30 generations - Real World Symbolic Regression

| Problem         | Hidden-Layers | Set   | DAE-GP         | Pre-Trained    | P-Value | Cliffs-Delta |
|-----------------|---------------|-------|----------------|----------------|---------|--------------|
| Airfoil         | 1             | Train | <b>12.6611</b> | 16.2778        | 0.57    | 0.16         |
|                 | 1             | Test  | <b>12.5944</b> | 16.2131        | 0.62    | 0.14         |
| Airfoil         | 2             | Train | <b>7.0644</b>  | 7.7109         | 0.62    | 0.14         |
|                 | 2             | Test  | <b>6.991</b>   | 7.6799         | 0.91    | 0.04         |
| Boston_Housing  | 2             | Train | <b>8.0217</b>  | 8.0543         | 0.85    | 0.06         |
|                 | 2             | Test  | <b>7.9472</b>  | 7.9683         | 0.79    | 0.08         |
| Energy(Cooling) | 2             | Train | <b>4.449</b>   | 4.4668         | 0.54    | 0.17         |
|                 | 2             | Test  | <b>4.6258</b>  | 4.6429         | 0.76    | 0.09         |
| Concrete        | 2             | Train | 17.1299        | <b>16.9825</b> | 0.91    | -0.04        |

| Problem | Hidden-Layers | Set     | DAE-GP         | Pre-Trained | P-Value | Cliffs-Delta |
|---------|---------------|---------|----------------|-------------|---------|--------------|
| 2       | Test          | 17.1585 | <b>16.7413</b> | 0.62        | -0.14   |              |

## 5.2 Influence on Solution Size

Next I studied the size of solutions found during DAE-GP. Figure 23 shows the median size of the best solution per generation aggregated over all benchmark problems for symbolic regression.

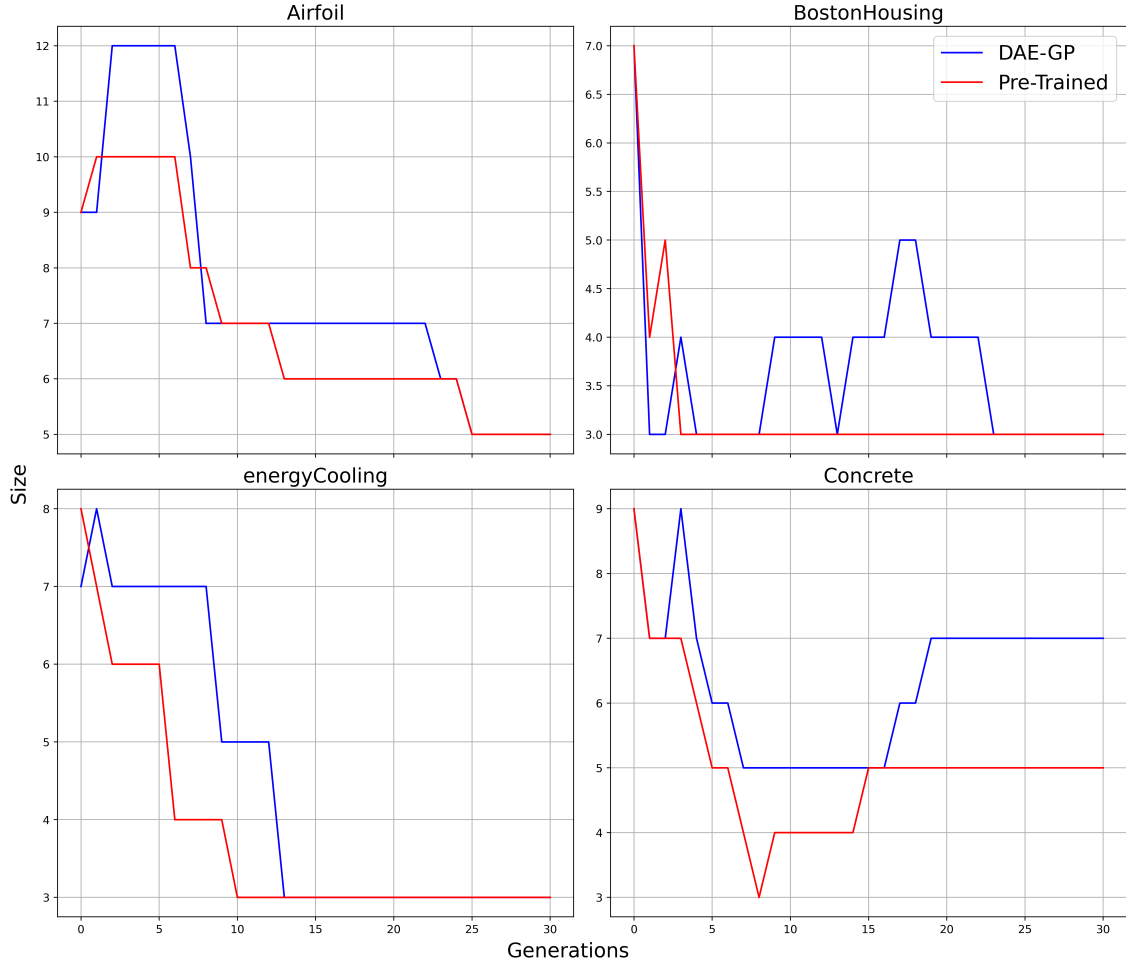


Figure 23: Size of the best Solution over 30 Generations - Real World Symbolic Regression

Table 6 shows the median size of the best solution after 30 generations and results for computing the statistical tests.

Table 6: Median Size of the best solution after 30 generations  
 - Real World Symbolic Regression

| Problem         | Hidden Layers | DAE-     |             | P-Value | Cliffs-Delta |
|-----------------|---------------|----------|-------------|---------|--------------|
|                 |               | GP       | Pre-Trained |         |              |
| Airfoil         | 1             | <b>5</b> | 7           | 0.44    | 0.20         |
| Airfoil         | 2             | 5        | 5           | 0.97    | -0.02        |
| Boston_Housing  | 2             | 3        | 3           | 0.37    | -0.20        |
| Energy(Cooling) | 2             | 3        | 3           | 0.21    | -0.28        |
| Concrete        | 2             | 7        | <b>5</b>    | 0.21    | -0.33        |

### 5.3 Influence on Population Diversity

Figure 24 shows the median levenshtein edit distance as a metric for population diversity over the evolutionary search. It clearly shows that pre-training does increase the population diversity for DAE-GP consistently for all tested benchmark problems.

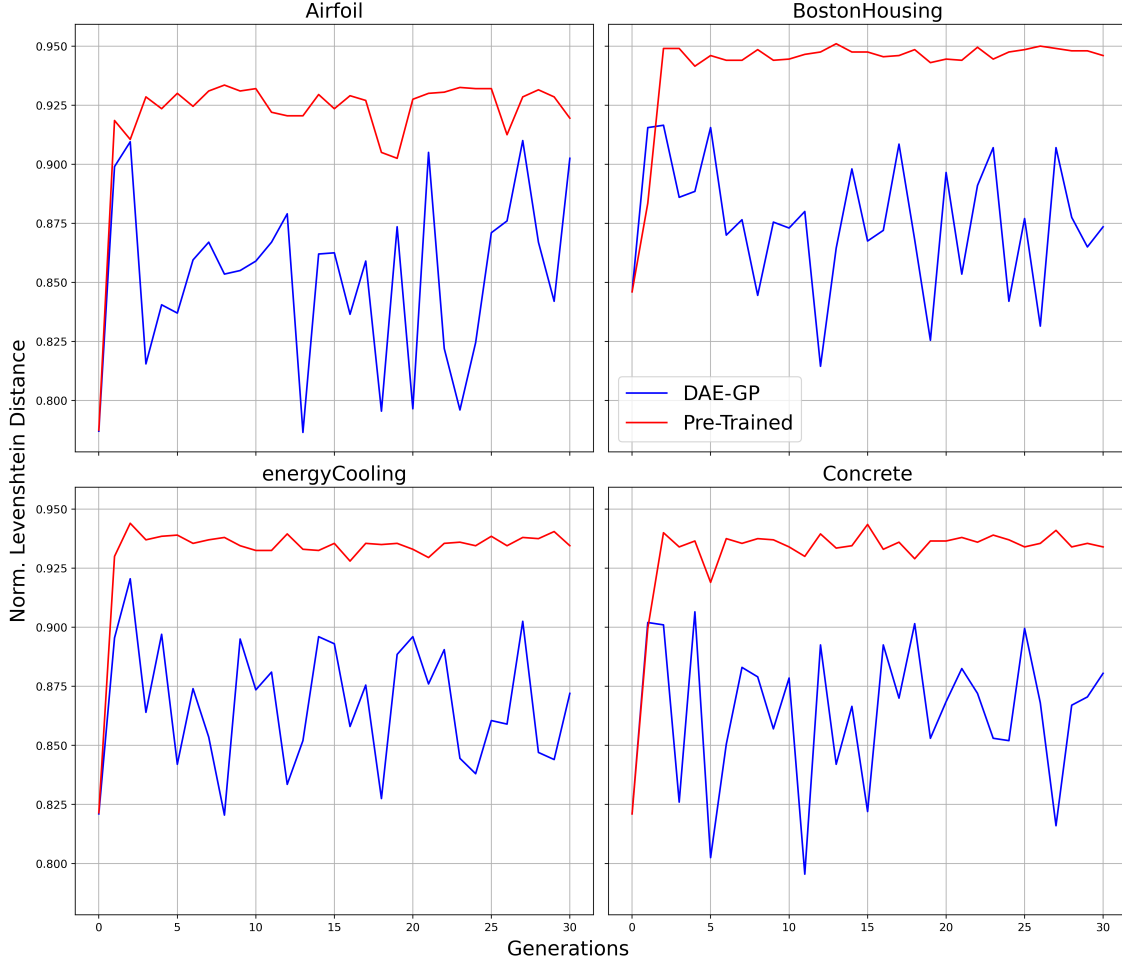


Figure 24: Population Diversity over 30 Generations - Real World Symbolic Regression

The results of the statistical analysis is summarized in table 7.

Table 7: Median Population Diversity over 30 Generations -  
Symbolic Regression

| Problem         | Hidden Layers | DAE- |             | P-Value | Cliffs-Delta |
|-----------------|---------------|------|-------------|---------|--------------|
|                 |               | GP   | Pre-Trained |         |              |
| Airfoil         | 1             | 0.86 | <b>0.93</b> | 0.00*** | 0.93         |
| Airfoil         | 1             | 0.86 | <b>0.93</b> | 0.00*** | 0.93         |
| Boston_Housing  | 1             | 0.88 | <b>0.95</b> | 0.00*** | 0.92         |
| Energy(Cooling) | 1             | 0.87 | <b>0.94</b> | 0.00*** | 0.94         |
| Concrete        | 1             | 0.87 | <b>0.94</b> | 0.00*** | 0.93         |

#### 5.4 Influence on the number of Training epochs per Generation

Figure 25 shows the median number of epochs spend on training each generations DAE-LSTM network until the termination criterion was satisfied.

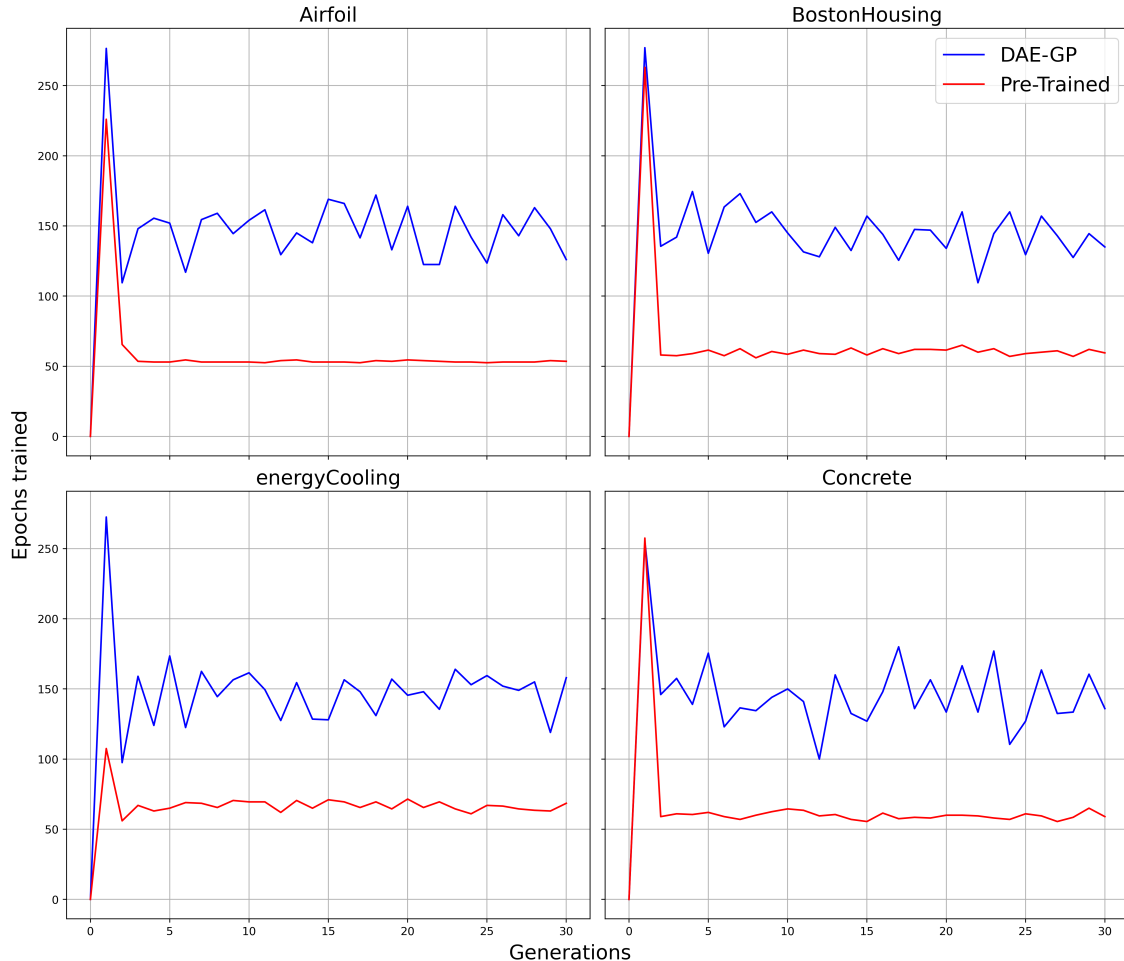


Figure 25: Training Epochs over 30 Generations - Real World Symbolic Regression

The results of the statistical analysis is summarized in table 8.

Table 8: Median Number of Training Epochs per Generation  
- Symbolic Regression

| Problem         | Hidden Layers | DAE-   |              | P-Value | Cliffs-Delta |
|-----------------|---------------|--------|--------------|---------|--------------|
|                 |               | GP     | Pre-Trained  |         |              |
| Airfoil         | 1             | 143.49 | <b>64.66</b> | 0.00*** | -0.88        |
| Airfoil         | 2             | 143.83 | <b>61.22</b> | 0.00*** | -0.88        |
| Boston_Housing  | 2             | 141.8  | <b>65.36</b> | 0.00*** | -0.87        |
| Energy(Cooling) | 2             | 144.24 | <b>66.7</b>  | 0.00*** | -0.93        |
| Concrete        | 2             | 139.2  | <b>65.15</b> | 0.00*** | -0.87        |

## 6 Conclusion and Discussion

### 6.1 Benefits of using Pre-Training

The experiments conducted in the scope of this master thesis did find that the implemented pre-training strategy resulted in an increased population diversity measured by the normalized levenshtein edit distance. Increasing the population diversity can be an important mechanism in controlling the search behavior of population based meta heuristics and is especially useful for increasing the exploration of the search space of possible solutions !QUELLE!.

Another significant benefit of using pre-training in DAE-GP is that it is highly efficient in decreasing the number of training epochs that are necessary to train each generations DAE-LSTM model. Even though pre-training increased the median total run-time for the tested benchmark problem in combination with the chosen DAE-LSTM dimensions, reducing the number of training epochs might be a possible way to lower the run time of DAE-GP if further performance optimizations, especially during model sampling, can be achieved.

### 6.2 Disadvantages of using Pre-Training

The experiments conducted in this thesis did not find any significant benefits on both solution quality as well as run-time for solving real world symbolic regression problems with pre-trained DAE-GP in comparison to regular DAE-GP.

As detailed in the subsection [Dynamic Adjustment of Hidden Neurons](#), one major drawback of using pre-training with DAE-GP is the loss of the ability to dynamically adjust the number of hidden neurons to the maximum size of individuals inside the current generations population. This dynamic mechanism does reduce the computational resources necessary for training DAE-LSTM networks which is one of the most time consuming operations besides sampling new individuals.

Another disadvantage of using pre-training in DAE-GP is that, in my experiments, it required DAE-LSTM networks to use two hidden layers (see subsection [Reduced Number of Hidden Layers](#)). For a single hidden layer, pre-training did show a negative impact on the median final fitness of solutions found as it was suggested by [4]. Since current research on DAE-GP for real-world symbolic regression relies on a single hidden layer (see [32]), pre-training does come with additional computational expenses for using deeper DAE-LSTMs.

### 6.3 Limitations and open Questions

One major limitation for the experiments conducted during the research phase of this thesis has been the large computational effort for experimenting with DAE-GP. Since single runs for DAE-GP have a run-time of many hours, it was not possible for me to extend the experiments to larger population sizes or more generations. Also I did not perform an extended optimization of hyperparameters (e.g by using a grid search strategy) which might yield configurations that increase the benefits of pre-training. As described in subsection [Influence on Run-Time](#), sampling new solutions has been a large contributor to the large performance hit on run-time by using pre-training. It could be a worthwhile endeavour to explore the main factors that increase sampling time for pre-trained DAE-GP to more efficiently exploit the benefits of pre-training like reducing the number of training epochs.

Another limitation of this research is the software implementation used for all experiments. As briefly touched in the subsection [Influence on Run-Time](#), I found some evidence that my implementation of pre-training suffered from increased run-time costs for internal error handling in the used `keras` library for deep neural networks. By optimizing the source code or even re-implementing it in a more performance-focused programming language (such as `C++` or `Rust`), large improvements to the pre-training strategy might be achievable.

Another possibility to improve the benefits of pre-training for DAE-GP is based on the findings of [5]. Pre-Training has shown to be especially useful for the lower layers of DAEs so it could be worthwhile to further experiment with only adapting the weights for a subset of the hidden layers inside the DAE-LSTM networks to either reduce run-time or to improve on the quality of solutions found during the evolutionary search.

## Nomenclature

### Symbols

Table 9: List of Mathematical Symbols

| Symbol            | Meaning   |
|-------------------|---|
| $g_n$             | $n$ .th generation  |
| $g_{max}$         | Maximum number of generations   |
| $M_g$             | DAE-LSTM model for generation $g$                                       |
| $\hat{M}$         | DAE-LSTM model for Pre-Training   |
| $\theta_M$        | Trainable parameters of DAE-LSTM model $M$                              |
| $P_g$             | Population of generation $g$  |
| $\hat{P}$         | Pre-Training Population   |
| $\hat{P}_{train}$ | Pre-Training Population used for training DAE-LSTM model $\hat{M}$      |
| $\hat{P}_{test}$  | Pre-Training Population used for validating DAE-LSTM model $\hat{M}$    |
| $X_g$             | Selected Training Population for DAE-LSTM model $M_g$ in generation $g$ |

### Abbreviations

Table 10: List of Abbreviations

| Abbreviation | Meaning  |
|--------------|--|
| DAE-GP       | Denoising Autoencoder Genetic Programming            |
| GP           | Genetic Programming                                  |
| EDA          | Estimation of Distribution Algorithm                 |
| EC           | Evolutionary Computation                             |
| DAE          | Denoising Autoencoder                                |
| DAE-LSTM     | Denoising Autoencoder Long Short Term Memory Network |
| RMSE         | Root Mean Squared Error                              |
| AQ           | Analytic Quotient                                    |

## References

- [1] Thomas F. Brooks, Dennis S. Pope, and Michael A. Marcolini. 1989. Airfoil self-noise and prediction.
- [2] Francois Chollet and others. 2015. Keras. Retrieved from <https://github.com/fchollet/keras>
- [3] Norman Cliff. 1993. Dominance statistics: Ordinal analyses to answer ordinal questions. *Psychological Bulletin* 114, (1993), 494–509.
- [4] Dumitru Erhan, Aaron Courville, Yoshua Bengio, and Pascal Vincent. 2010. Why does unsupervised pre-training help deep learning? In *Proceedings of the thirteenth international conference on artificial intelligence and statistics* (Proceedings of machine learning research), PMLR, Chia Laguna Resort, Sardinia, Italy, 201–208. Retrieved from <https://proceedings.mlr.press/v9/erhan10a.html>
- [5] Dumitru Erhan, Pierre-Antoine Manzagol, Yoshua Bengio, Samy Bengio, and Pascal Vincent. 2009. The difficulty of training deep architectures and the effect of unsupervised pre-training. In *Proceedings of the twelth international conference on artificial intelligence and statistics* (Proceedings of machine learning research), PMLR, Hilton Clearwater Beach Resort, Clearwater Beach, Florida USA, 153–160. Retrieved from <https://proceedings.mlr.press/v5/erhan09a.html>
- [6] Félix-Antoine Fortin, François-Michel De Rainville, Marc-André Gardner, Marc Parizeau, and Christian Gagné. 2012. DEAP: Evolutionary algorithms made easy. *Journal of Machine Learning Research* 13, (July 2012), 2171–2175.
- [7] Xu Han, Zhengyan Zhang, Ning Ding, Yuxian Gu, Xiao Liu, Yuqi Huo, Jiezhong Qiu, Yuan Yao, Ao Zhang, Liang Zhang, Wentao Han, Minlie Huang, Qin Jin, Yanyan Lan, Yang Liu, Zhiyuan Liu, Zhiwu Lu, Xipeng Qiu, Ruihua Song, Jie Tang, Ji-Rong Wen, Jinhui Yuan, Wayne Xin Zhao, and Jun Zhu. 2021. Pre-trained models: Past, present and future. *AI Open* 2, (2021), 225–250. DOI:[https://doi.org/https://doi.org/10.1016/j.aiopen.2021.08.002](https://doi.org/10.1016/j.aiopen.2021.08.002)
- [8] Charles R. Harris, K. Jarrod Millman, Stéfan J. van der Walt, Ralf Gommers, Pauli Virtanen, David Cournapeau, Eric Wieser, Julian Taylor, Sebastian Berg, Nathaniel J. Smith, Robert Kern, Matti Picus, Stephan Hoyer, Marten H. van Kerkwijk, Matthew Brett, Allan Haldane, Jaime Fernández del Río, Mark Wiebe, Pearu Peterson, Pierre Gérard-Marchant, Kevin Sheppard, Tyler Reddy, Warren Weckesser, Hameer Abbasi, Christoph Gohlke, and Travis E. Oliphant. 2020. Array programming with NumPy. *Nature* 585, 7825 (September 2020), 357–362. DOI:<https://doi.org/10.1038/s41586-020-2649-2>
- [9] David Harrison and Daniel Rubinfeld. 1978. Hedonic housing prices and the demand for clean air. *Journal of Environmental Economics and Management* 5, (March 1978), 81–102. DOI:[https://doi.org/10.1016/0095-0696\(78\)90006-2](https://doi.org/10.1016/0095-0696(78)90006-2)
- [10] G. E. Hinton and R. R. Salakhutdinov. 2006. Reducing the dimensionality of data with neural networks. *Science* 313, 5786 (2006), 504–507. DOI:<https://doi.org/10.1126/science.1127647>
- [11] Sepp Hochreiter and Jürgen Schmidhuber. 1997. Long short-term memory. *Neural computation* 9, (December 1997), 1735–80. DOI:<https://doi.org/10.1162/neco.1997.9.8.1735>
- [12] J. D. Hunter. 2007. Matplotlib: A 2D graphics environment. *Computing in Science & Engineering* 9, 3 (2007), 90–95. DOI:<https://doi.org/10.1109/MCSE.2007.55>
- [13] Diederik P. Kingma and Jimmy Ba. 2014. Adam: A method for stochastic optimization. *CoRR* abs/1412.6980, (2014).

- [14] John R. Koza. 1993. Genetic programming - on the programming of computers by means of natural selection. In *Complex adaptive systems*.
- [15] Joseph B. Kruskal. 1983. An overview of sequence comparison: Time warps, string edits, and macromolecules. *SIAM Rev.* 25, 2 (April 1983), 201–237. DOI:<https://doi.org/10.1137/1025045>
- [16] Henry B. Mann and Douglas R. Whitney. 1947. On a test of whether one of two random variables is stochastically larger than the other. *Annals of Mathematical Statistics* 18, (1947), 50–60.
- [17] Ji Ni, Russ H. Driberg, and Peter I. Rockett. 2013. The use of an analytic quotient operator in genetic programming. *IEEE Transactions on Evolutionary Computation* 17, 1 (February 2013), 146–152. DOI:<https://doi.org/10.1109/TEVC.2012.2195319>
- [18] Sinno Jialin Pan and Qiang Yang. 2010. A survey on transfer learning. *IEEE Transactions on Knowledge and Data Engineering* 22, 10 (2010), 1345–1359. DOI:<https://doi.org/10.1109/TKDE.2009.191>
- [19] Grégory Paris, Denis Robilliard, and Cyril Fonlupt. 2004. Exploring overfitting in genetic programming. In *Artificial evolution*, Springer Berlin Heidelberg, Berlin, Heidelberg, 267–277.
- [20] Fernando Pérez and Brian E. Granger. 2007. IPython: A system for interactive scientific computing. *Computing in Science and Engineering* 9, 3 (May 2007), 21–29. DOI:<https://doi.org/10.1109/MCSE.2007.53>
- [21] Malte Probst and Franz Rothlauf. 2020. Harmless overfitting: Using denoising autoencoders in estimation of distribution algorithms. *Journal of Machine Learning Research* 21, 78 (2020), 1–31. Retrieved from <http://jmlr.org/papers/v21/16-543.html>
- [22] Franz Rothlauf. 2011. *Design of modern heuristics: Principles and application*. DOI:<https://doi.org/10.1007/978-3-540-72962-4>
- [23] Dirk Schweim, David Wittenberg, and Franz Rothlauf. 2021. On sampling error in genetic programming. *Natural computing* 2021, (2021). DOI:<https://doi.org/http://doi.org/10.25358/openscience-5820>
- [24] The pandas development team. 2020. Pandas-dev/pandas: pandas. DOI:<https://doi.org/10.5281/zenodo.3509134>
- [25] Athanasios Tsanas and Angeliki Xifara. 2012. Accurate quantitative estimation of energy performance of residential buildings using statistical machine learning tools. *Energy and Buildings* 49, (June 2012), 560–567. DOI:<https://doi.org/10.1016/j.enbuild.2012.03.003>
- [26] Guido Van Rossum and Fred L. Drake. 2009. *Python 3 reference manual*. CreateSpace, Scotts Valley, CA.
- [27] Pascal Vincent, Hugo Larochelle, Y. Bengio, and Pierre-Antoine Manzagol. 2008. Extracting and composing robust features with denoising autoencoders. In *Proceedings of the 25th international conference on machine learning* (ICML '08), Association for Computing Machinery, New York, NY, USA, 1096–1103. DOI:<https://doi.org/10.1145/1390156.1390294>

- [28] Pauli Virtanen, Ralf Gommers, Travis E. Oliphant, Matt Haberland, Tyler Reddy, David Cournapeau, Evgeni Burovski, Pearu Peterson, Warren Weckesser, Jonathan Bright, Stéfan J. van der Walt, Matthew Brett, Joshua Wilson, K. Jarrod Millman, Nikolay Mayorov, Andrew R. J. Nelson, Eric Jones, Robert Kern, Eric Larson, C J Carey, İlhan Polat, Yu Feng, Eric W. Moore, Jake VanderPlas, Denis Laxalde, Josef Perktold, Robert Cimrman, Ian Henriksen, E. A. Quintero, Charles R. Harris, Anne M. Archibald, Antônio H. Ribeiro, Fabian Pedregosa, Paul van Mulbregt, and SciPy 1.0 Contributors. 2020. SciPy 1.0: Fundamental Algorithms for Scientific Computing in Python. *Nature Methods* 17, (2020), 261–272. DOI:<https://doi.org/10.1038/s41592-019-0686-2>
- [29] Andreas Weigend. 1994. On overfitting and the effective number of hidden units. In *Proceedings of the 1993 connectionist models summer school*, 335–342.
- [30] Frank. Wilcoxon. 1945. Individual comparisons by ranking methods. *Biometrics* 1, (1945), 196–202.
- [31] David Wittenberg. 2022. Using denoising autoencoder genetic programming to control exploration and exploitation in search. In *Genetic programming*, Springer International Publishing, Cham, 102–117.
- [32] David Wittenberg and Franz Rothlauf. 2022. Denoising autoencoder genetic programming for real-world symbolic regression. In *Proceedings of the genetic and evolutionary computation conference companion (GECCO '22)*, Association for Computing Machinery, New York, NY, USA, 612–614. DOI:<https://doi.org/10.1145/3520304.3528921>
- [33] David Wittenberg, Franz Rothlauf, and Dirk Schweim. 2020. DAE-GP: Denoising autoencoder LSTM networks as probabilistic models in estimation of distribution genetic programming. In *Proceedings of the 2020 genetic and evolutionary computation conference (GECCO '20)*, Association for Computing Machinery, New York, NY, USA, 1037–1045. DOI:<https://doi.org/10.1145/3377930.3390180>
- [34] I-Cheng Yeh. 1998. Modeling of strength of high-performance concrete using artificial neural networks.” cement and concrete research, 28(12), 1797-1808. *Cement and Concrete Research* 28, (December 1998), 1797–1808. DOI:[https://doi.org/10.1016/S0008-8846\(98\)00165-3](https://doi.org/10.1016/S0008-8846(98)00165-3)

## **Statutory Declaration**

... hier einfügen...